https://doi.org/10.5194/acp-2020-784
Preprint. Discussion started: 14 September 2020

Atmospheric Chemistry and Physics Discussions

Organosulfates in atmospheric aerosols in Shanghai, China: seasonal and interannual variability, origin, and formation mechanisms

Yao Wang[1], Yue Zhao[1,2,*], Yuchen Wang[3], Jian-Zhen Yu[3,4], Jingyuan Shao[5], Ping Liu[1], Wenfei Zhu[1], Zhen Cheng[1], Ziyue Li[1], Naiqiang Yan[1,2], Huayun Xiao[1]

[1]School of Environmental Science and Engineering, Shanghai Jiao Tong University, Shanghai 200240, China

[2]Shanghai Institute of Pollution Control and Ecological Security, Shanghai 200092, China

[3]Division of Environment & Sustainability, Hong Kong University of Science & Technology, Hong Kong, China

[4]Department of Chemistry, Hong Kong University of Science & Technology, Hong Kong, China

[5]College of Flight Technology, Civil Aviation University of China, Tianjin 300300, China

*Corresponding author: Yue Zhao (yuezhao20@sjtu.edu.cn)

https://doi.org/10.5194/acp-2020-784
Preprint. Discussion started: 14 September 2020

Atmospheric Chemistry and Physics Discussions

Abstract

Organosulfates (OS) are ubiquitous in the atmosphere and serve as important tracers for secondary organic aerosols (SOA). Despite intense research over years, the abundance, origin, and formation mechanisms of OS in ambient aerosols, in particular in regions with severe anthropogenic pollution, are still not well understood. In this study, we collected filter samples of ambient fine particulate matter ($PM_{2.5}$) over four seasons in both 2015/2016 and 2018/2019 at an urban site in Shanghai, China, and comprehensively characterized the OS species in these $PM_{2.5}$ samples using a liquid chromatography coupled to a high resolution mass spectrometer (UPLC-ESI-QToF-MS). We find that while the concentration of organic aerosol (OA) decreased by 29% in 2018/2019, compared to that in 2015/2016, the annually averaged concentrations of 35 quantified OS were similar in two years (65.5±77.5 ng m^{-3} in 2015/2016 versus 59.4±79.7 ng m^{-3} in 2018/2019), suggesting an increased contribution of SOA to OA in 2018/2019 than in 2015/2016. Isoprene- and monoterpene-derived OS are the two most abundant OS families, on average accounting for 36.3% and 31.0% of the quantified OS concentrations, respectively, suggesting an important contribution of biogenic emissions to the production of OS and SOA in Shanghai. The abundance of biogenic OS, particularly those arising from isoprene, exhibited strong seasonality (peaked in summer) but no significant interannual variability. In contrast, anthropogenic OS such as diesel-derived ones had little seasonal variability and declined obviously in 2018/2019 compared with that in 2015/2016. This reflects a significant change in precursor emissions in eastern China in recent years. The C_2/C_3 OS species that have both biogenic and anthropogenic origins averagely contributed to 19.0% of the quantified OS, with $C_2H_3O_6S^-$, $C_3H_5O_5S^-$, and $C_3H_5O_6S^-$ being the most abundant ones, together accounting for 76% of C_2/C_3 OS concentrations. 2-Methyltetrol sulfate (2-MT-OS, $C_5H_{11}O_7S^-$) and monoterpene-derived $C_{10}H_{16}NO_7S^-$ were the most abundant OS and nitrooxy-OS in summer, contributing to 31% and 5% of the quantified OS, respectively. The substantially larger concentration ratio of 2-MT-OS to 2-methylglyceric acid sulfate (2-MA-OS, $C_4H_7O_7S^-$) in summer (6.8-7.8) than in other seasons (0.31-0.78) implies that low-NOx oxidation pathways played a dominant role in isoprene-derived SOA formation in summer, while high-NOx reaction pathways were more important in other seasons. We further find that the production of OS was largely controlled by the level of Ox ($O_x = O_3 + NO_2$), namely, the photochemistry of OS precursors, in particular in summer, though sulfate concentration, aerosol acidity, as well as aerosol liquid water content (ALWC) that could affect the heterogeneous chemistry of reactive intermediates leading to OS formation also played a role. Our study provides valuable insights into the characteristics and mechanisms of OS formation in a typical Chinese megacity and implies that mitigation of Ox pollution can effectively reduce the production of OS and SOA in eastern China.

https://doi.org/10.5194/acp-2020-784
Preprint. Discussion started: 14 September 2020

Atmospheric Chemistry and Physics Discussions

1 Introduction

Secondary organic aerosol (SOA) accounts for a significant fraction of atmospheric fine particulate matter ($PM_{2.5}$) (Jimenez et al., 2009; Huang et al., 2014) and contributes significantly to deteriorated air quality and Earth's climate forcing (Ramanathan et al., 2001; Mahowald, 2011; Huang et al., 2014; Shrivastava et al., 2017). SOA consists of thousands of organic compounds that are diverse in molecular properties. Identification and quantification of the composition of SOA are essential for understanding the composition, the chemistry of formation and evolution, properties, and climate and health impacts of SOA (Hoffmann et al., 2011; Nozière et al., 2015). However, currently only a small portion of organic matters in SOA are identified as specific compounds (Hoffmann et al., 2011; Nozière et al., 2015; Johnston and Kerecman, 2019). Organosulfates (OS) are important constituents of SOA and have been frequently detected in both polluted and clean environments (Iinuma et al., 2007a; Surratt et al., 2008; Claeys et al., 2010; Froyd et al., 2010; Hawkins et al., 2010; Hatch et al., 2011; Lin et al., 2012a; Stone et al., 2012; Hansen et al., 2014; He et al., 2014; Ma et al., 2014; Tao et al., 2014; Liao et al., 2015; Shakya and Peltier, 2015; Kourtchev et al., 2016; Meade et al., 2016; Wang et al., 2016b; Hettiyadura et al., 2017; Huang et al., 2018; Le Breton et al., 2018; Wang et al., 2018; Hettiyadura et al., 2019; Wang et al., 2019a). It has been estimated that OS accounted for 6-12% of total sulfur in a rural area in K-puszta, Hungary (Lukacs et al., 2009), 1.3% of fine particulate organic mass (POM) in Fairbanks, Alaska (Shakya and Peltier, 2013), and 1-13% of fine POM across the continental United States (Tolocka and Turpin, 2012; Shakya and Peltier, 2015). Studies have also shown that OS can affect aerosol properties such as acidity, viscosity, hygroscopicity, and light-absorbing properties (Nguyen et al., 2012; Hansen et al., 2015; Estillore et al., 2016; DeRieux et al., 2018; Fleming et al., 2019; Olson et al., 2019; Riva et al., 2019).

Chamber studies have revealed that OS can originate from the (photo)oxidation of both biogenic precursors such as isoprene (Surratt et al., 2007a; Surratt et al., 2007b; Gómez-González et al., 2008), monoterpenes (Iinuma et al., 2007a; Iinuma et al., 2007b; Surratt et al., 2007a; Surratt et al., 2008; Iinuma et al., 2009), sesquiterpenes (Chan et al., 2011), and 2-methyl-3-buten-2-ol (Zhang et al., 2012), as well as anthropogenic precursors such as polycyclic aromatic hydrocarbons, long-chain alkanes, naphthenes (Riva et al., 2015; Riva et al., 2016b), and diesel and biodiesel fuel vapors (Blair et al., 2017) in the presence of sulfate aerosol or SO_2. Many of OS observed in these chamber studies have also been detected in ambient atmosphere, among which isoprene- and monoterpene-derived OS are usually most abundant in forested, rural, and even urban areas (Surratt et al., 2008; Hatch et al., 2011; Kristensen and Glasius, 2011; Stone et al., 2012; He et al., 2014; Ma et al., 2014; Kourtchev et al., 2016; Meade et al., 2016; Hettiyadura et al., 2017; Hettiyadura et al., 2019; Wang et al., 2019a).

In addition to the precursors, detailed formation mechanisms of OS have also been widely studied. The acid-catalyzed ring-opening reaction of epoxides was established to be an important mechanism for the formation of OS (Iinuma et al., 2009; Surratt et al., 2010; Lin et al., 2012b; Zhang et al., 2014), in particular for isoprene-derived OS (Surratt et al., 2010; Hatch et al., 2011; Lin et al., 2012b). 2-Methyltetrol sulfate (2-MT-OS, $C_5H_{11}O_7S^-$), formed via reactive uptake of isoprene epoxide (IEPOX) on sulfate, is one of the most abundant OS in atmospheric aerosol (Chan et al., 2010; Liao et al., 2015), which can contribute up to 12.6% of the organic carbon mass in Atlanta, GA (Hettiyadura et al., 2019). Another OS formation pathway is the nucleophilic substitution of tertiary organonitrates by inorganic sulfate. Darer et al. (2011) found that tertiary organonitrates are thermodynamically unstable and can undergo nucleophilic substitution with sulfate to generate OS rapidly.

https://doi.org/10.5194/acp-2020-784
Preprint. Discussion started: 14 September 2020


Atmospheric Chemistry and Physics Discussions

This mechanism can also explain the formation of some nitrooxy-OS (NOS). In atmospheric aqueous phase, sulfate radicals that can be produced by oxidation of S(IV) species in the presence of transition metal ions (TMI) (Grgic et al., 1998; Herrmann, 2003) or by OH radical reaction with bisulfate (Jiang et al., 1992; Herrmann, 2003) can also react with unsaturated organic compounds to form OS. Laboratory studies have shown that a large number of OS were produced by the bulk aqueous-phase oxidation of isoprene or its oxidation products, methyl vinyl ketone (MVK) and methacrolein (MACR), in the presence of inorganic sulfate or peroxodisulfate under irradiation (Nozière et al., 2010; Schindelka et al., 2013), or in the presence of S(IV) and TMI under dark conditions (Huang et al., 2019). However, field observational evidence for this mechanism is still lacking. In addition, reactive uptake of SO_2 on organic aerosol can also result in the production of OS. Laboratory studies have found that sulfur dioxide (SO_2) could react with C=C bond in unsaturated fatty acids under dark conditions to form OS (Shang et al., 2016). Such OS have been detected in ambient atmosphere with an estimated contribution of 0.3‰-0.9‰ to OM in $PM_{2.5}$ in southern China (Zhu et al., 2019). Recent studies have also shown efficient production of OS from heterogeneous/aqueous-phase reactions of SO_2 with organic peroxide-containing aerosol and SOA (Wang et al., 2019b; Yao et al., 2019). Such OS production was found to be mainly a result of the direct reaction between SO_2 and peroxides, rather than acid-catalyzed reaction involving inorganic sulfate (Wang et al., 2019b). Currently, the acid-catalyzed ring-opening reaction of IEPOX has been the most well-studied mechanism and proved to be important in atmospheric OS formation by both field and modelling studies (Chan et al., 2010; Surratt et al., 2010; Hatch et al., 2011; McNeill et al., 2012; Pye et al., 2013; Worton et al., 2013; Kourtchev et al., 2016; He et al., 2018; Hettiyadura et al., 2019). However, atmospheric importance of other OS formation mechanisms remains to be evaluated.

The OS formation pathways aforementioned can be affected by aerosol properties such as acidity, aerosol liquid water content (ALWC), and sulfate concentration. There is ample evidence from laboratory studies that increased aerosol acidity significantly enhances the production of OS from acid-catalyzed reactions (Iinuma et al., 2007b; Surratt et al., 2007a; Surratt et al., 2007b; Chan et al., 2011; Zhang et al., 2012), while field studies have shown that the abundance of OS was not or only weakly correlated with aerosol acidity in some locations (Nguyen et al., 2014; Budisulistiorini et al., 2015; Brüggemann et al., 2017; Rattanavaraha et al., 2017), suggesting the existence of other factors (e.g., ALWC, sulfate content, etc.) that control OS formation in these areas. ALWC has dual effects on OS formation. On one hand, elevated ALWC can reduce the viscosity and/or inhibit the liquid-liquid phase separation of aerosol, which would favor the dissolution and mixing of reactive intermediates such as IEPOX and multifunctional aldehydes in aqueous sulfate aerosol (Shiraiwa et al., 2011; McNeill et al., 2012; Liao et al., 2015) or SO_2 in organic aerosol (Passananti et al., 2016; Shang et al., 2016; Yao et al., 2019), thereby enhancing OS formation. On the other hand, high ALWC would decrease aerosol acidity via dilution, hence inhibiting the acid-catalyzed OS formation. High ALWC may also promote the hydrolysis of OS in aqueous aerosol (Darer et al., 2011).

Quantification of OS is important for understanding their abundance and the chemistry of formation and evolution in the atmosphere. Owing to the lack of authentic standards, the quantification of OS remains a challenging task. Recently, several research groups have synthesized a series of authentic standards (e.g., glycolic acid sulfate, lactic acid sulfate, hydroxyacetone sulfate, 2-methyltetrol sulfate, benzyl sulfate, α-pinene sulfate, β-pinene sulfate, and limonene sulfate) that are structurally the same or similar with the OS found in atmospheric aerosols (Olson et al., 2011; Kundu et al., 2013; Staudt et al., 2014; Budisulistiorini et al., 2015; Hettiyadura et al., 2015; Wang et al., 2017; Huang et al., 2018). They used these authentic

https://doi.org/10.5194/acp-2020-784
Preprint. Discussion started: 14 September 2020


Atmospheric Chemistry and Physics Discussions

standards to quantify OS in ambient aerosols and provided important constraints on the abundance, origin, and chemistry of OS in the atmosphere.

Up to date, there are few studies characterizing atmospheric OS in areas with severe anthropogenic pollution. Situated in the eastern Yangtze River Delta (PRD) of China, Shanghai has a population of more than 24 million and is plagued by air pollution (Behera et al., 2015; Wang et al., 2016a). Here we conducted a comprehensive investigation of the molecular composition, abundance, sources, and formation processes of OS in ambient aerosols in Shanghai. More than 150 ambient $PM_{2.5}$ samples collected over four seasons during both 2015/2016 and 2018/2019 in urban Shanghai were analyzed using an ultra-performance liquid chromatography quadrupole time-of-flight mass spectrometer (UPLC-QToF-MS), and 35 OS were quantified using 7 synthesized and commercially purchased OS standards. Seasonal and interannual variations of OS, in response to the changes in emissions, meteorological conditions, and $PM_{2.5}$ chemical compositions, were comprehensively characterized, and the influencing factors such as aerosol acidity, ALWC, sulfate content, oxidant level and so on for OS formation were probed. This study would help to understand the characteristics and mechanisms of OS and SOA production under the strong influence of anthropogenic pollution in Chinese megacities.

2 Materials and methods

2.1 Ambient Sample collection

In total 156 ambient $PM_{2.5}$ samples were collected from 8 April 2015 to 16 January 2016 and from 23 October 2018 to 5 August 2019 in Shanghai, China. The sampling site is located on the rooftop of a 20-meter-tall teaching building on the Xuhui Campus of Shanghai Jiao Tong University, which is in downtown and surrounded by residential and commercial areas (see Fig. 1a, b). There is a main street 230 m east to the sampling site. The $PM_{2.5}$ samples were collected on pre-baked (550 ℃, 8 h) quartz-fiber filters (Whatman) from 9:00 am to 8:00 am of the next day using a high-volume sampler (HiVol 3000, Ecotech) at a flow rate of 67.8 m^3 h^{-1}. The collected samples were wrapped in pre-baked (550 ℃, 8 h) aluminum foil and stored at -20 ℃ before analysis.

2.2 Organosulfate measurement with UPLC-ESI-ToF-MS

An aliquot of ~17 cm^2 was removed from each filter sample and extracted in 3 mL of methanol (LC-MS grade, CNW Technologies GmbH) twice under sonication in an ice bath for 30 min. The extracts derived each time were combined and filtered through a 0.45 μm PTFE syringe filter (CNW Technologies GmbH) to remove insoluble materials, and subsequently concentrated to 250 μL with a gentle stream of ultra-high-purity nitrogen (Shanghai Likang Gas Co., Ltd). The resulting extracts were mixed with ultrapure water (milliQ, 18.2 MΩ·cm) of the same volume and centrifugated to get supernatant for analysis.

The resulting solutions were analyzed using an Acquity UPLC (Waters) coupled to a Xevo G2-XS QToF-MS (Waters) having a mass resolving power of ≥ 40000 and equipped with an electrospray ionization (ESI) source. The analytes were separated by a BEH C_{18} column (2.1×100 mm, 1.7 μm particle size) at 50 ℃. A gradient elution procedure was performed using methanol (A) and water (B) both containing 0.1% acetic acid (v/v) as the eluents: A was maintained at 99% for 1.5 min, decreased to 46% in 6.5 min and to 5% in 3 min, then decreased to 1% in 1 min and held for 2 min, finally returned to 99%

https://doi.org/10.5194/acp-2020-784
Preprint. Discussion started: 14 September 2020


Atmospheric Chemistry and Physics Discussions

in 0.5 min and held for 1.5 min to equilibrate the column. The total eluent flow rate was 0.33 mL min^{-1} and the sample injection volume was 2.0 μL. The ESI source was operated under optimum conditions as follows: capillary voltage 2.0 kV, sampling cone voltage 40 V, source offset voltage 80 V, source temperature 115°C, desolvation gas temperature 450°C, cone gas 50 L h^{-1}, desolvation gas 900 L h^{-1}.

The quantified OS as well as the authentic and surrogate standards used for the quantification of each OS are listed in Table 1. The OS standards were selected by mainly referring to Hettiyadura et al. (2019), which is based upon a comparison of the MS/MS pattern between authentic standards and targeted OS in ambient aerosols, as well as to Wang et al (2018). Glycolic acid sulfate (GAS) and lactic acid sulfate (LAS) were synthesized according to Olson et al. (2011). The purities of GAS and LAS are 8% and 15 %, respectively, determined by ^{1}H NMR analysis using dichloroacetic acid as an internal standard. Limonaketone sulfate and α-pinene sulfate were synthesized and details were described in Wang et al. (2017). Other OS standards including sodium methyl sulfate (99%, Macklin), sodium octyl sulfate (95%, Sigma-Aldrich), and potassium phenyl sulfate (98%, Tokyo Chemical Industry, Shanghai) were commercially purchased. The quantified OS were also analyzed in tandem mass spectrometry (MS/MS) in negative (-) ion mode at a collision energy of 10-50 eV to confirm whether they are OS by sulfur-containing fragment ions observed. In this study, most quantified OS were fragmented to the bisulfate anion (m/z 97) and several quantified OS were only fragmented to the sulfate radical anion (m/z 96) and the sulfite radical anion (m/z 80) (see Fig. S1).

2.3 Auxiliary measurements

Meteorological parameters, including temperature, relative humidity (RH), and wind speed (WS) were continuously monitored by Shanghai Hongqiao international airport station, which is 9 km west to the sampling site (Fig. 1c). The concentrations of SO_2, nitrogen dioxide (NO_2), O_3 and $PM_{2.5}$ were measured by a state-controlled air quality monitoring station on the Xuhui Campus of Shanghai Normal University, which is 4.5 km southwest to the sampling site for the $PM_{2.5}$ filter samples (Fig. 1c). Organic carbon (OC) and elemental carbon (EC) in $PM_{2.5}$ filter samples were measured by a thermal-optical multiwavelength carbon analyzer (DRI Model 2015). The concentration of organic matter (OM) was derived by multiplying the OC by 1.6 (Tao et al., 2017). Water-soluble inorganic compounds including sulfate, nitrate, chloride, ammonium, potassium, and calcium were analyzed with an ion chromatograph (Metrohm MIC).

2.4 Estimation of aerosol liquid water content and pH

The ISORROPIA-II thermodynamic model (Fountoukis and Nenes, 2007) was employed to predict ALWC and aerosol pH. The aerosol water-soluble inorganic ion concentrations, as well as temperature and RH were used as the model input. The model was run in the forward model for metastable aerosol, which was shown to give a more accurate representation of aerosol pH than using the reverse-mode calculations when with only aerosol data input (Guo et al., 2015; Hennigan et al., 2015). ISORROPIA-II calculates the equilibrium concentration of aerosol hydronium ions (H^{+}_{air}) per volume of air (μg m^{-3}), along with ALWC (μg m^{-3}). The aerosol pH was then derived by

$$\mathrm{pH} = -\log_{10}\left(\mathrm{H}^{+}_{\mathrm{aq}}\right) = -\log_{10}\frac{1000\mathrm{H}^{+}_{\mathrm{air}}}{\mathrm{ALWC}}, \qquad (1)$$

https://doi.org/10.5194/acp-2020-784
Preprint. Discussion started: 14 September 2020

Atmospheric Chemistry and Physics Discussions

where H^{+}_{aq} is the concentration of hydronium ions in aqueous aerosol (mol L^{-1}). In this study, ALWC associated with organic aerosol and its influences on aerosol pH were not considered. However, previous studies showed that water uptake by organic aerosol only contributed to a minor fraction (5%) of total ALWC and had a negligible influence on aerosol pH in haze events in China (Liu et al., 2017).

2.5 Quality control

The extraction efficiency of OS species in filter samples was evaluated by measuring the recovery of different OS standards. The synthesized and commercially purchased OS standards were spiked into blank and pre-baked quartz filters, followed by extraction and analysis with the same procedures for ambient samples. The recoveries of OS standards were about 84-94% except for Δ-Carene OS, the recovery of which was 66% (see Table S1). This result suggests a fairly high extraction efficiency for the majority of OS species in this study.

In addition, we evaluated the matrix effect on the signal response of OS by comparing the measured signal intensity of OS standards added to the extracts of ambient $PM_{2.5}$ filter samples with that of pure OS standard solutions. Table S2 gives the ratios of measured signal intensity of OS standards in filter sample extracts to that in pure solutions. Most of OS standards had a ratio around 1, suggesting no obvious matrix effect on the measurement of the majority of OS species. However, the two smallest OS standards, methyl sulfate and glycolic acid sulfate that were the very first species eluted from LC column, had a ratio significantly smaller than 1, suggesting the inhibited ionization of these two OS likely by the highly soluble and polar species in the filter samples that were co-eluted with these two OS. We note that the matrix effect for these two OS is dependent on the $PM_{2.5}$ mass loading. For example, the signal ratio of glycolic acid sulfate standard measured in filter sample extracts versus in pure solutions ranged from 0.17-0.31 (Exps. 1-2) for very polluted days to 0.45-0.53 for clean days (Exps. 3-4). This implies that the abundance of glycolic acid sulfate in ambient aerosols reported here may be underestimated by a factor of 2-6 due to the matrix effect.

3 Results and Discussion

3.1 Overview of pollution characteristics during sampling periods

Figure 2 shows the time series of meteorological parameters, O_3, NO_2, SO_2, $PM_{2.5}$ and its major components, as well as H^{+}_{aq} and ALWC during the sampling periods. The average values (concentrations) of each parameter (species) were given in Table S3. The meteorological conditions (wind speed, temperature, and RH) were overall similar in 2015/2016 and 2018/2019. While the NO_2 concentration decreased from 27.0±13.0 ppb in 2015/2016 to 21.3±10.3 ppb in 2018/2019, the O_3 level had no obvious difference in two years (29.8±15.2 ppb in 2015/2016 versus 29.6±13.9 ppb in 2018/2019), consistent with the nonlinear response of O_3 production to precursor emissions (Liu and Wang, 2020). The annual average mass loading of $PM_{2.5}$ declined by 34.5% in 2018/2019 (38.6±24.0 μg m^{-3}) compared to that 2015/2016 (59.0±37.9 μg m^{-3}), largely driven by the strong decrease in the abundance of OM (29.1%) and sulfate (37.4%). The decrease of $PM_{2.5}$, OM, and sulfate concentrations from 2015/2016 to 2018/2019 reflects a significant reduction in anthropogenic pollutant emissions in eastern China in recent years. In contrast to OM and sulfate, the concentration of nitrate had little change between 2015/2016 (8.8±8.9 μg m^{-3}) and 2018/2019 (8.4±7.8 μg m^{-3}), despite an obvious decrease in NO_2 concentration. This is at least partly a result of reduced

https://doi.org/10.5194/acp-2020-784
Preprint. Discussion started: 14 September 2020

Atmospheric Chemistry and Physics Discussions

aerosol acidity (H^+_{aq}, see Fig. 2 and Table S3) and thereby enhanced partitioning of HNO_3 into the particle phase. Furthermore, the nitrate concentration showed a strong seasonality, ranging from 1.0±1.1 and 3.4±3.2 μg m^{-3} in summer to 16.6±10.0 and 14.1±10.0 μg m^{-3} in winter in 2015/2016 and 2018/2019, respectively, partly owing to the seasonal variation of temperature and aerosol acidity that modulates the gas/particle partitioning of nitrate (Fisseha et al., 2006; Griffith et al., 2015; Guo et al., 2015; Guo et al., 2016). A similar strong reduction in $PM_{2.5}$ concentration and variations in aerosol composition over the past several years were observed in different regions in China (Tao et al., 2017; Wen et al., 2018; Ding et al., 2019a; Wang et al., 2020b). As a result of strong reductions in inorganic ion concentrations, ALWC decreased dramatically in 2018/2019 (14.8±20.4 μg m^{-3}), compared to that in 2015/2016 (24.4±27.0 μg m^{-3}). In short, anthropogenic pollutant emissions, as well as aerosol concentration and composition varied significantly between 2015/2016 and 2018/2019 in Shanghai, which, as will be discussed below, has important implications for the production of OS in ambient aerosols.

3.2 Molecular composition of sulfur-containing organic compounds

The organic compounds in ambient $PM_{2.5}$ identified using UPLC-ESI(-)-QToF-MS were classified into four groups based on their elemental composition, i.e., CHO, CHON, CHOS, and CHONS. Figure 3a, b show the average mass spectra of organic compounds in $PM_{2.5}$ over a typical winter (21-26 January 2019) and summer (23-28 July 2019) pollution episode. The S-containing compounds were overall larger in molecular size than CHO and CHON compounds, likely because of the addition of a sulfate group to the molecule. The molecular weight (MW) of most S-containing compounds was between 100-400 Da, and a few between 400-700 Da. The high-MW CHOS species showed a larger contribution in winter than in summer, suggesting that they are more likely to arise from anthropogenic sources than biogenic emissions. Figure 3c shows the signal contribution of different compound categories as well as concentrations of sulfate, OM, and quantified OS, and Fig. 3d, e shows the number of identified organic compounds in each category during two pollution episodes. The CHOS compounds contributed most by signal and number to observed organic compounds in both winter and summer. The signal contributions and number of unquantified CHOS and CHONS did not vary significantly from winter to summer, whereas the signal contribution of quantified CHOS and CHONS species were significantly larger in summer than in winter (on average 15% vs. 7% for CHOS and 11% vs. 7% for CHONS). As will be discussed later, the abundance of quantified anthropogenic OS was fairly constant across different seasons, in striking contrast to biogenic OS that showed strong seasonal variability. Therefore, lack of seasonal variability for unquantified CHOS and CHONS implies that they may originate mainly from anthropogenic sources. In addition, both signal intensity and the number of CHO species increased significantly in summer, compared to those in winter. In contrast, CHON compounds contributed substantially more to the observed signals in winter than in summer (on average 25% vs. 7%), though their numbers are quite similar during the two periods. This suggests an enhanced production and/or suppressed depletion of nitrogen-containing organic species in winter.

The CHOS compounds with an O/S ratio of ≥ 4 were assigned as potential OS species. Similarly, the CHONS compounds with an O/(N+S) ratio of ≥ 7 could be assigned as potential NOS species (Lin et al., 2012a). The $C_8H_{17}O_4S^-$, $C_8H_{15}O_4S^-$, and $C_{27}H_{53}O_{11}S^-$ were the highest OS peaks observed in the pollution episode in winter. The $C_8H_{17}O_4S^-$ and $C_8H_{15}O_4S^-$ species may be derived from the photooxidation of diesel fuel vapors according to previous chamber studies (Blair et al., 2017). The highest NOS peak in winter is $C_{10}H_{16}NO_7S^-$, which likely originate from monoterpene oxidation (Surratt et al., 2008). The

https://doi.org/10.5194/acp-2020-784
Preprint. Discussion started: 14 September 2020


Atmospheric Chemistry and Physics Discussions

$C_5H_{11}O_7S^-$, $C_{15}H_{29}O_5S^-$, and $C_{13}H_{25}O_5S^-$ were observed among the highest OS peaks in the summer pollution episode. The $C_5H_{11}O_7S^-$ is an IEPOX-derived OS species (Surratt et al., 2010), while $C_{15}H_{29}O_5S^-$ and $C_{13}H_{25}O_5S^-$ may be derived from the oxidation of diesel fuel vapors (Blair et al., 2017). The highest NOS peak in summer is monoterpene-derived $C_{10}H_{16}NO_7S^-$, the same with that in winter.

3.3 Quantified organosulfates

In this study, we quantified twenty-nine OS and six NOS compounds using a variety of authentic and surrogate OS standards (Table 1). The quantified OS and NOS accounted for 14-18% and 47-67% by intensity of identified CHOS and CHONS, respectively, in polluted winter days and 15-37% and 58-87%, respectively, in polluted summer days (Fig. 3c). Increased contribution of the quantified OS and NOS in summer is because they are mainly derived from biogenic VOCs, which have greater emissions in summer than in other seasons (Guenther et al., 1995). We note that a large fraction of OS signals were not quantified owing to the lack of proper standards in this study. As discussed above, these unquantified OS mainly originated from anthropogenic sources. Future studies of their abundances and formation mechanisms are warranted.

Table 2 summarizes the seasonally and annually averaged concentrations of the quantified OS, as well as their contributions to OM in 2015/2016 and 2018/2019. The average concentration of quantified OS was 65.5±77.5 ng m^{-3} in 2015/2016 and 59.4±79.7 ng m^{-3} in 2018/2019. Although there was little change in OS concentration in these two years, the contribution of OS to OM was larger in 2018/2019 (0.66%±0.56%) than in 2015/2016 (0.57%±0.56%), mainly due to a significant reduction of OM in 2018/2019. Since OS species are important tracers for SOA (Surratt et al., 2007b; Gómez-González et al., 2008; Surratt et al., 2008; Surratt et al., 2010; McNeill et al., 2012; Zhang et al., 2012; Lin et al., 2013), an increase of OS/OM ratios in 2018/2019 implies an enhanced contribution of SOA to OA in Shanghai. A previous study by Ma et al. (2014) reported an average OS concentration in urban Shanghai in 2012/2013 of about 8.6 ng m^{-3}, substantially smaller than the concentration reported here. This is likely due to a different number of OS species quantified (17 vs. 35) and different OS standards used (octyl and benzyl sulfates vs. seven authentic/surrogate standards) in Ma et al. (2014) and the present study. As can be seen in Fig. 2e and Table 2, the OS concentration and OS/OM ratio both showed a strong seasonal variation and peaked in summer. The concentration of OS and its contribution to OM in summertime Shanghai (on average, 114.1 ng m^{-3} and 1.13% in July 2015 and 102.1 ng m^{-3} and 1.18% in July 2019) were larger or comparable to those observed in Beijing (55.2 ng m^{-3}, 0.42%) (Wang et al., 2018), Centreville, AL (54.7 ng m^{-3}, 0.24%) (Hettiyadura et al., 2017), and Birmingham, Alabama (205.4 ng m^{-3}, 2%) (Rattanavaraha et al., 2017), but significantly lower than those observed in Atlanta (2366.4 ng m^{-3}, 16.5%) (Hettiyadura et al., 2019) where the production of OS and SOA is dominated by the oxidation of biogenic emissions. The contribution of OS to OM in wintertime Shanghai (on average, 0.32% in January 2016 and 0.36% in January 2019) was larger than that observed in Xi'an (~0.2%) (Huang et al., 2018), though the quantified OS concentrations in two regions were comparable. This may suggest a stronger secondary formation of OA in Shanghai than in Xi'an, consistent with independent measurements by Huang et al. (2014).

To further characterize the seasonality and interannual variability of OS, as well as their origin and formation mechanisms, the quantified OS were assigned to four different source categories based on their molecular composition and literature data (Surratt et al., 2007a; Surratt et al., 2008; Nozière et al., 2010; Surratt et al., 2010; Schindelka et al., 2013; Zhang et al., 2014;

https://doi.org/10.5194/acp-2020-784
Preprint. Discussion started: 14 September 2020


Atmospheric Chemistry and Physics Discussions

Riva et al., 2015; Riva et al., 2016b; Blair et al., 2017; Nestorowicz et al., 2018). The OS species for each OS source category are listed in Table 1 and the seasonal and interannual variations in the abundance of grouped and individual OS are shown in Fig. 4 and Table S4, respectively.

3.3.1 Isoprene-derived organosulfates

Isoprene-derived OS (hereafter referred to as OS_i) include ten $C_{4\text{-}5}$ species and one dimeric species ($C_7H_9O_7S$). The average concentration of OS_i in summer was 76.5±93.4 ng m^{-3} for 2015/2016 and 68.4±102.2 ng m^{-3} for 2018/2019, significantly larger than the concentrations (10.4-17.1 ng m^{-3}) in other seasons (Fig. 4a). Similar strong seasonality of OS_i was also observed in suburban areas in the Mid-Atlantic United States (Meade et al., 2016) and the Pearl River Delta in Southern China (He et al., 2014) The significantly increased production of OS_i in summer is mainly a result of enhanced isoprene emissions (Guenther et al., 1995) and photochemistry due to strong solar radiation and high temperatures in this warmer season.

The most abundant species among OS_i was 2-MT-OS ($C_5H_{11}O_7S^-$), produced by reactive uptake of IEPOX on sulfate during the photooxidation of isoprene under low-NOx conditions (Surratt et al., 2010). The average concentration of 2-MT-OS was ~31 ng m^{-3} in summer, contributing to about 45% of OS_i, whereas it decreased to 0.4-1.3 ng m^{-3} in other seasons, accounting for only 4-10% of OS_i (see Table S4). In addition, 2-methylglyceric acid sulfate (2-MA-OS, $C_4H_7O_7S^-$) was also abundantly detected with an average concentration of 4.5 ng m^{-3} in summer and 1.0-2.2 ng m^{-3} in other seasons. 2-MA-OS is formed from reactive uptake of methacrylic acid epoxide (MAE) (Lin et al., 2013) and hydroxymethyl-methyl-lactone (HMML) (Nguyen et al., 2015) on sulfate aerosol during isoprene photooxidation under high-NOx conditions. It is worthwhile noting that the concentration ratio of 2-MT-OS/2-MA-OS in summer (6.8-7.8) is substantially larger than that in other seasons (0.31-0.78). This is consistent with a dramatic reduction of NOx level (e.g., NO_2) in summer (~13 ppb) compared to that in other seasons (~24-34 ppb) (see Table S3). Furthermore, the NOx-influenced oxidation pathways may not be conducive to 2-MA-OS formation in summer, given that the formation of reactive intermediates such as MAE is unfavorable at high temperatures owing to enhanced thermal decomposition of its precursor methacryloylperoxynitrate (MPAN) (Worton et al., 2013). Since 2-MT-OS and 2-MA-OS are key tracers for isoprene-derived SOA under low- and high-NOx conditions, respectively (Surratt et al., 2010; Lin et al., 2013; Nguyen et al., 2015). The dramatically larger ratios of 2-MT-OS/2-MA-OS in summer than in other seasons therefore strongly suggests that the low-NOx oxidation pathways dominated the production of isoprene-derived SOA in summer, while the processes favorable under high-NOx conditions were important SOA formation in other seasons. We note that the 2-MT-OS/2-MA-OS ratios observed in summertime Shanghai are smaller than those (17.0-33.8) observed in less polluted environments such as the southeastern United States (Budisulistiorini et al., 2015; Hettiyadura et al., 2019; Riva et al., 2019), but significantly larger than those (0.55-1.57) observed in Beijing (Wang et al., 2018; Bryant et al., 2020) and the Pearl River Delta (PRD) region of China (He et al., 2018).

Other abundant OS_i species include $C_5H_7O_7S^-$, $C_5H_9O_7S^-$, and $C_4H_7O_6S^-$. The $C_5H_7O_7S^-$ and $C_5H_9O_7S^-$ species can be produced by photooxidation of isoprene (Surratt et al., 2008; Nestorowicz et al., 2018) and/or the oxidative aging of methyltetrol sulfate (Hettiyadura et al., 2015). The $C_4H_7O_6S^-$ can be generated both from sulfate radical reaction with MACR/MVK (Nozière et al., 2010; Schindelka et al., 2013; Wach et al., 2019) and isoprene photooxidation (Surratt et al., 2007a; Lin et al., 2013; Nestorowicz et al., 2018). The $C_5H_7O_7S^-$ and $C_4H_7O_6S^-$ are also consistent in molecular formula with the OS species formed

https://doi.org/10.5194/acp-2020-784
Preprint. Discussion started: 14 September 2020


Atmospheric Chemistry and Physics Discussions

from the photooxidation of diesel fuel vapors (Blair et al., 2017). However, these two species had moderate to strong correlations with MT-OS and $C_5H_9O_7S^-$ in different seasons expect for autumn ($C_5H_7O_7S^-$: r=0.68-0.96, $C_4H_7O_6S^-$: r=0.62-0.96), indicating that they are mainly derived from isoprene oxidation. We note that the five most abundant OS_i species as discussed above were moderately correlated with EC and CO in winter (r=0.5-0.67), suggesting that there might be anthropogenic sources of isoprene in winter. Borbon et al. (2001) measured the hourly isoprene concentration at an urban site in Lille, France for two years and found that isoprene was largely derived from vehicle emissions in winter. In addition to OS species, two isoprene-derived NOSs ($C_5H_{10}NO_9S^-$ and $C_5H_8NO_{10}S^-$) were also observed, in particular in summer.

3.3.2 Monoterpene-derived organosulfates

Monoterpene-derived OS (hereafter referred to as OS_m) include seven $C_{7\text{-}10}$ OS species and three $C_{9\text{-}10}$ NOS species. Compared to the OS_i, the OS_m showed a weaker seasonal variation and a relatively larger abundance except in summer (Fig. 4b). This is consistent with the fact that isoprene emissions have stronger seasonal variability than monoterpene emissions (Guenther et al., 1995). The seasonally averaged concentrations of OS_m were higher in spring and summer, but lower in autumn and winter. This is different from previous observations in 2012/2013 in Shanghai by Ma et al (2014). They found that the OS_m were most abundant in summer, followed by autumn, winter, and spring. The differences in seasonal variations of OS_m observed by the two studies may be attributed to different meteorological and chemical conditions that affected precursor emissions and chemistry of OS_m formation over the sampling periods. Given that the OS_m concentration had an obvious daily variation, the number of samples collected would significantly affect the seasonally averaged concentration. As such, the difference in the number of samples collected each season (18-20 samples in this study versus 6 samples within three days in Ma et al. (2014)) may also contribute to the different seasonality observed in two studies.

The NOS species such as $C_{10}H_{16}NO_7S^-$, $C_9H_{14}NO_8S^-$, and $C_{10}H_{16}NO_{10}S^-$ were the most abundant OS_m species, which arises mainly from monoterpenes photooxidation in the presence of NOx or nighttime NO_3 chemistry (Iinuma et al., 2007a; Surratt et al., 2008). The concentrations of these three NOS were all lower in summer than in spring and autumn (Table S4), consistent with the seasonal trend of NOx concentrations (Fig. 2 and Table S3). Similar seasonal variations for these NOS species were also observed in the PRD region of China (He et al., 2014) and the Mid-Atlantic United States (Meade et al., 2016). Among NOS species, the $C_{10}H_{16}NO_7S^-$ was most abundant, contributing to 22-48% of OS_m. This species had an annual average concentration of 6.2±6.5 ng m^{-3} in 2015/2016 and 5.5±6.2 ng m^{-3} in 2018/2019, which is comparable to the concentrations observed in Beijing (12 ng m^{-3}) (Wang et al., 2018) and Atlanta (9.0 ng m^{-3}) (Hettiyadura et al., 2019), but much lower than observed in the PRD region of China (52.4 ng m^{-3} in summer and 151 ng m^{-3} in autumn) (He et al., 2014). The prevalence of monoterpene-derived NOS in Shanghai as observed in this study is consistent with recent observations that monoterpenes accounted for up to 60% of nighttime NO_3 radical loss in the YRD region of China (Wang et al., 2020a).

The most abundant nitrogen-free OS_m species was $C_{10}H_{15}O_7S^-$ (m/z 279.0538), which was shown to be produced from the photooxidation of monoterpenes (Surratt et al., 2008) or sulfate radical reaction with α-pinene (Nozière et al., 2010). Although the $C_{10}H_{15}O_7S^-$ is consistent in molecular composition with the OS species formed by photooxidation of cyclodecane in the presence of sulfate aerosol (Riva et al., 2016b), its moderate to strong correlation (r=0.51-0.93) with the three monoterpene-derived NOS in all seasons except for winter suggests that it is mainly derived from monoterpene oxidation. The concentration

https://doi.org/10.5194/acp-2020-784
Preprint. Discussion started: 14 September 2020

Atmospheric Chemistry and Physics Discussions

of $C_{10}H_{15}O_7S^-$ was on average 3.0 ± 3.0 ng m^{-3} in 2015/2016, lower than that (4.0 ± 3.4 ng m^{-3}) in 2018/2019. In contrast to NOS species, the $C_{10}H_{15}O_7S^-$ species was most abundant in summer in both years, again suggesting a strong contribution of low-NOx chemistry in OS and SOA formation in summer.

3.3.3 Anthropogenic organosulfates

The quantified anthropogenic OS (hereafter referred to as OS_a) in this study include phenyl sulfate ($C_6H_5O_4S^-$), benzyl sulfate ($C_7H_7O_4S^-$), $C_8H_{17}O_4S^-$, as well as $C_4H_7O_4S^-$, $C_5H_7O_6S^-$, and $C_6H_9O_6S^-$. The annual average concentrations of OS_a in 2015/2016 and 2018/2019 were 5.6±2.8 ng m^{-3} and 3.8±3.3 ng m^{-3}, respectively. The decreased concentrations of OS_a in 2018/2019 is consistent with a significant reduction of anthropogenic pollutant emissions in China in recent years. Since only a small fraction of OS_a were quantified in this study, the OS_a concentration was substantially smaller compared to biogenic OS. In addition, the OS_a concentration had little seasonal variations in both 2015/2016 and 2018/2019 (Fig. 4c). Among quantified OS_a, the $C_4H_7O_4S^-$ was most abundant with an annual average concentration of 2.0±1.5 ng m^{-3} in 2015/2016 and 1.8±2.6 ng m^{-3} in 2018/2019, which is comparable to the concentrations in Atlanta (Hettiyadura et al., 2019). Blair et al. (2017) found that photooxidation of diesel vapors in the presence of SO_2 can form $C_4H_7O_4S^-$, $C_5H_7O_6S^-$, and $C_6H_9O_6S^-$ species. The $C_8H_{17}O_4S^-$ species had the same retention time with the octyl sulfate standard in the LC column, suggesting it is a long-chain aliphatic OS. This OS species was correlated with $C_5H_7O_6S^-$ and $C_6H_9O_6S^-$ that were potential diesel vapor-derived OS. Phenyl sulfate and benzyl sulfate may be produced by photooxidation of naphthalene and 2-methylnaphthalene (Riva et al., 2015), but phenyl sulfate was only detected in 42 out of 75 samples in 2015/2016 and 8 out of 81 samples in 2018/2019, primarily in winter. The benzyl sulfate concentrations in 2015/2016 and 2018/2019 were 0.4±0.1 ng m^{-3} and 0.2±0.10 ng m^{-3}, respectively, which were higher than the observations in springtime Lahore, Pakistan (Staudt et al., 2014) and in wintertime Xi'an, China (Huang et al., 2018). Benzyl sulfate had a strong correlation with phenyl sulfate and was also correlated with $C_6H_9O_6S^-$ and $C_8H_{17}O_4S^-$.

3.3.4 C_2/C_3 organosulfates

The OS species with two or three carbon atoms are grouped together since many of them are considered to have both biogenic and anthropogenic origins. The C_2/C_3 OS quantified in this study include $C_2H_3O_6S^-$ (m/z 154.9650), $C_3H_5O_5S^-$ (m/z 152.9858), $C_3H_5O_6S^-$ (m/z 168.9807), $C_2H_3O_5S^-$ (m/z 138.9701), $C_3H_5O_4S^-$ (m/z 136.9909), and $C_3H_7O_5S^-$ (m/z 155.0014). The C_2/C_3 OS species averagely accounted for 19% of quantified OS concentrations and they were overall more abundant in summer than in other seasons (Fig. 4d). The $C_2H_3O_6S^-$, $C_3H_5O_5S^-$, and $C_3H_5O_6S^-$ species, which were previously assigned to glycolic acid sulfate (GAS), hydroxyacetone sulfate (HAS), and lactic acid sulfate (LAS), respectively (Olson et al., 2011; Hettiyadura et al., 2017; Huang et al., 2018; Wang et al., 2018; Hettiyadura et al., 2019), were among the most abundant C_2/C_3 OS species, together contributing to 76% of C_2/C_3 OS concentrations. The concentration of $C_2H_3O_6S^-$ (GAS) was on average 2.9±2.2 ng m^{-3} in 2015/2016 and 2.3±1.7 ng m^{-3} in 2018/2019, which was lower than the concentrations measured in Beijing (19.5 ng m^{-3}) (Wang et al., 2018), Xi'an (77.3 ng m^{-3}) (Huang et al., 2018), Atlanta (58.5 ng m^{-3}) (Hettiyadura et al., 2019), Centreville (20.6 ng m^{-3}) (Hettiyadura et al., 2017), Lahore, Pakistan (11.3 ng m^{-3}), and Bakersfield, CA (4.5-5.4 ng m^{-3}) (Olson et al., 2011), and similar with those observed in Riverside, CA (3.3 ng m^{-3}) (Olson et al., 2011). We note that if accounting for the underestimation (2-6 times) in concentration due to matrix effects (see Sect. 2.5), the GAS concentration measured in

https://doi.org/10.5194/acp-2020-784
Preprint. Discussion started: 14 September 2020

Atmospheric Chemistry and Physics Discussions

Shanghai would be comparable to that in most of the regions mentioned above. The concentrations of $C_3H_5O_5S^-$ (HAS) and $C_3H_5O_6S^-$ (LAS) were quite similar, on average 2.3 and 2.2 ng m^{-3} in 2015/2016 and 1.8 and 1.9 ng m^{-3} in 2018/2019, respectively, which were comparable to the concentrations observed in Beijing (2.2 ng m^{-3} and 4.4 ng m^{-3}) (Wang et al., 2018), and Xi'an (1.3 ng m^{-3} for HAS) (Huang et al., 2018), but lower than those measured in Centreville (5.8 ng m^{-3} and 16.5 ng m^{-3}) (Hettiyadura et al., 2017) and Atlanta (10.1 ng m^{-3} and 38.4 ng m^{-3}) (Hettiyadura et al., 2019). The $C_2H_3O_6S^-$, $C_3H_5O_5S^-$, $C_3H_5O_6S^-$, and $C_2H_3O_5S^-$ were strongly correlated with most of OS_I species (r=0.52-0.96 for $C_2H_3O_6S^-$, r=0.53-0.99 for $C_3H_5O_5S^-$, r=0.53-0.90 for $C_3H_5O_6S^-$, and r=0.53-0.94 for $C_2H_3O_5S^-$), indicating that they originated mainly from isoprene chemistry. This is in line with recent findings that a series of C_2/C_3 OS species, including $C_2H_3O_6S^-$, $C_3H_5O_6S^-$, and $C_2H_3O_5S^-$, can be produced by heterogeneous OH oxidation of particulate 2-MT-OS (Chen et al., 2020). The $C_3H_5O_4S^-$ species, proposed to contain an allyl group (Hettiyadura et al., 2017), was previously found to be produced by diesel photooxidation (Blair et al., 2017), and was correlated with anthropogenic OS such as the potential diesel vapor-derived OS ($C_8H_{17}O_4S^-$, $C_4H_7O_4S^-$, $C_5H_7O_6S^-$, and $C_6H_9O_6S^-$, r=0.53-0.87) and benzyl sulfate ($C_7H_7O_4S^-$, r=0.49-0.88). The $C_3H_7O_5S^-$ is likely an OS species containing one hydroxyl group (Hettiyadura et al., 2017), which was strongly correlated with the $C_3H_5O_4S^-$ in all seasons and correlated with the diesel vapor-derived OS_a ($C_6H_9O_6S^-$ and $C_8H_{17}O_4S^-$) in spring and autumn, suggesting that it may be largely derived from the photooxidation of diesel vapors. This result is different from the observations in Atlanta, where the $C_3H_7O_5S^-$ was correlated with most of OS_i, leading to the suggestion that it was derived from the oxidation of isoprene (Hettiyadura et al., 2019). We note that the concentrations of $C_3H_5O_4S^-$ and $C_3H_7O_5S^-$ species decreased significantly from 2015/2016 to 2018/2019 (except for summer, see Table S4), overall consistent with the interannual variations of OS_a species. This further supports that these two OS species mainly originated from anthropogenic sources.

3.4 Factors influencing organosulfate formation

Laboratory and field studies have shown that aerosol properties such as acidity, sulfate concentration, and ALWC play important roles in the formation of OS (Iinuma et al., 2007b; Surratt et al., 2007a; Surratt et al., 2007b; Chan et al., 2011; Liao et al., 2015; Hettiyadura et al., 2019; Riva et al., 2019). Here we examined the influences of these factors, as well as the level of oxidants and temperature on OS formation in ambient aerosols in Shanghai. Aerosol pH and ALWC here were calculated using ISORROPIA-II (see Sect. 2.4). Figure 5 shows the OS concentration versus the O_x level, sulfate concentration, aerosol pH, and ALWC observed in the spring, autumn, and winter of 2015-2016 and 2018-2019. Since the OS concentrations in summer were significantly greater than in other seasons, they were plotted separately in Fig. 6. As shown in Figs. 5 and 6, the aerosol pH in Shanghai ranged between 1.5 and 5.3 in summer and between 2.5 and 6.1 in other seasons, overall within the pH range (2-6) reported for ambient aerosols in northern China (Liu et al., 2017; Shi et al., 2017; Wang et al., 2018; Ding et al., 2019b; Song et al., 2019). The lower aerosol pH in summer than in other seasons was mainly a result of enhanced sulfate (decreased nitrate) mass fraction in aerosols (Fig. 2d) and decreased ALWC (Figs. 5 and 6c, d). Decreased aerosol pH in summer compared to other seasons were also observed in Beijing (Ding et al., 2019b) and the southeastern United States (Guo et al., 2015; Nah et al., 2018).

As can be seen in Fig. 5, the OS concentration in spring, autumn, and winter increased obviously with increasing Ox level, sulfate concentration, and aerosol acidity (Fig. 5a, b). A similar result was also found in Beijing that most OS species were

https://doi.org/10.5194/acp-2020-784
Preprint. Discussion started: 14 September 2020

Atmospheric Chemistry and Physics Discussions

correlated strongly with the product of ozone and particulate sulfate ($[O_3]\cdot[SO_4^{2-}]$) (Bryant et al., 2020). In addition, an overall positive correlation was observed between the OS concentration and ALWC (Fig. 5c, d). Therefore, it is likely that that the OS species were mainly produced by acid-catalyzed heterogeneous/aqueous-phase reactions of oxidized organic compounds with sulfate in these seasons. Previous studies have shown that elevated ALWC could inhibit OS production by decreasing aerosol acidity through dilution (Lewandowski et al., 2015; Nestorowicz et al., 2018). However, as the increase of ALWC was accompanied by elevated sulfate concentration, such a decrease in aerosol acidity was not observed in the present study (Fig. 5c, d). Alternatively, the increased ALWC likely promoted the mass transfer of oxidized organics into the aerosol phase, thereby enhancing OS formation. We note that the observations with moderate to high ALWC but relatively low OS concentration (data points in the triangle in Fig. 5c, d) were associated with low Ox levels (<50 ppb) that significantly limited the oxidation of VOC precursors and hence the formation of OS.

As seen in Fig. 6, OS production in summer increased dramatically with rising Ox concentration. In addition, high OS concentrations were associated with high ambient temperatures, which can enhance emissions of biogenic precursors and the production of Ox. While the aerosol acidity effect on OS production in summer was still evident, the influence of sulfate and ALWC was not as obvious as in other seasons. This is likely because the OS production in summer was driven by the strong emission and fast photochemistry of VOC precursors. It is noteworthy that the sulfate concentrations, ALWC, and aerosol acidities were overall higher in 2015/2016 than in 2018/2019, but the OS concentrations were similar in two years. This implies that the Ox level is a driving factor for OS formation in ambient aerosols in Shanghai. Very recently, a similar oxidant effect on OS formation was also observed in urban Beijing (Bryant et al., 2020). Therefore, mitigation of Ox pollution may effectively reduce the production of OS and SOA in Chinese megacities.

4 Conclusions

In this study, we collected ambient $PM_{2.5}$ filter samples over four seasons in 2015/2016 and 2018/2019 in urban Shanghai, China, and comprehensively characterized the sulfur-containing organic compounds (CHOS and CHONS) in these $PM_{2.5}$ samples using UPLC-ESI(-)-QToF-MS. The CHOS and CHONS species accounted for a large fraction of ion signals for organic compounds in ambient $PM_{2.5}$. Using a set of authentic and surrogate OS standards, we quantified the abundance of 29 OS and 6 NOS species in ambient aerosols. We find that there was no strong change in the OS concentration in 2018/2019 (59.4±79.7 ng m^{-3}) compared to that in 2015/2016 (65.5±77.5 ng m^{-3}), though the OM concentration decreased by 29% between 2015/2016 (12.7±8 μg m^{-3}) and 2018/2019 (9±5.5 μg m^{-3}). As a result, the annual average contribution of quantified OS to OM increased from 0.57% in 2015/2016 to 0.66% in 2018/2019, suggesting an enhanced contribution of SOA to OM in Shanghai in recent years. Isoprene- and monoterpene-derived organosulfates (OS_i and OS_m) accounted for 36.3% and 31.0% of the quantified OS concentrations, respectively, indicating a significant contribution of biogenic emissions to SOA in Shanghai. The abundance of OS_i had strong seasonality and was significantly higher in summer (76.5±93.4 ng m^{-3} in 2015/2016 and 68.4±102.2 ng m^{-3} in 2018/2019) than in other seasons (10.4-17.1 ng m^{-3}). The OS_m concentration showed a weaker seasonal variation and was relatively higher in spring and summer than in autumn and winter. In contrast, anthropogenic OS (OS_a) had little seasonal variations and decreased by 32% from 2015/2016 to 2018/2019 due to a significant reduction of anthropogenic pollutant emissions in recent years. The C_2/C_3 OS species that were more abundant in summer

https://doi.org/10.5194/acp-2020-784
Preprint. Discussion started: 14 September 2020

Atmospheric Chemistry and Physics Discussions

than in other seasons, on average contributed to 19% of the concentration of quantified OS species. The $C_2H_3O_6S^-$ (GAS), $C_3H_5O_5S^-$ (HAS), and $C_3H_5O_6S^-$ (LAS), which were derived mainly from isoprene chemistry, were the most abundant C_2/C_3 OS species and together accounted for 76% of C_2/C_3 OS concentrations.

2-MT-OS was the most abundant OS species in summer. The dramatic larger 2-MT-OS/2-MA-OS ratios in summer (6.8-7.8) versus other seasons (0.31-0.78) implies that the reaction pathways prevalent under low-NOx conditions (e.g., reactive uptake of IEPOX and photooxidation of ISOPOOH) dominated the production of OS_i and isoprene-derived SOA in summer, while the processes favorable under high-NOx conditions play an important role in OS_i and SOA formation in other seasons. The $C_{10}H_{16}NO_7S^-$ species derived from monoterpenes was the most abundant NOS species, with an annual average concentration of 6.2±6.5 ng m^{-3} in 2015/2016 and 5.5±6.2 ng m^{-3} in 2018/2019. This agrees well with previous observations that monoterpenes depleted about 60% of nighttime NO_3 radicals in the YRD region of China (Wang et al., 2020a).

In addition, we find that the abundance of OS is overall positively correlated with the O_x level, sulfate concentration, aerosol acidity, as well as ALWC in spring, autumn, and winter, suggesting the production of OS via acid-catalyzed aqueous-phase reactions of oxidized organic compounds on sulfate. However, OS production in summer was strongly driven by rising Ox and temperature that could enhance the photochemistry and emissions of biogenic precursors. We further find that although sulfate concentrations, aerosol acidities, and ALWC were significantly lower in 2018/2019 than in 2015/2016, the production of OS was largely sustained in 2018/2019 by the nearly unchanged Ox level that maintained the fast oxidation of VOC precursors. These results imply that controlling Ox pollution may also effectively mitigate particulate organic matter pollution in eastern China.

It should be pointed out that GAS was likely underestimated by a factor of 2-6 as a result of the matrix effect during the analysis in our study. If accounting for this effect, it would be the second most abundant OS species after MT-OS. In addition, a large fraction of CHOS signals that arose mainly from anthropogenic sources were not quantified due to the lack of proper OS standards in this study. Therefore, the OS concentration and its contribution to organic aerosol in Shanghai could be significantly greater. Future studies on the abundance, origin, and formation mechanisms of these unquantified OS are warranted for a better understanding of the formation and evolution of OS and SOA in the atmosphere.

Data availability. The data presented in this work are available upon request from the corresponding author Y. Zhao (yuezhao20@sjtu.edu.cn).

Author contributions. YZ designed and led the research, YW, WFZ, and ZC collected ambient samples, YCW and JZY provided OS standards, JYS conducted ISORROPIA-II model calculation, YW conducted sample analysis, and YZ and YW processed the data and wrote the paper with contributions from all of the authors.

Competing interests. The authors declare no conflict of interest.

Acknowledgments. This work was supported by the National Natural Science Foundation of China (Grant 21806104), the Science and Technology Commission of Shanghai Municipality (Grant 19DZ1205004), and the Program for Professor of Special Appointment (Eastern Scholar) at Shanghai Institutions of Higher Learning.

https://doi.org/10.5194/acp-2020-784
Preprint. Discussion started: 14 September 2020

Atmospheric Chemistry and Physics Discussions

References

Behera, S. N., Cheng, J., Huang, X., Zhu, Q., Liu, P., and Balasubramanian, R.: Chemical composition and acidity of size-fractionated inorganic aerosols of 2013-14 winter haze in Shanghai and associated health risk of toxic elements, Atmos. Environ., 122, 259-271, doi: 10.1016/j.atmosenv.2015.09.053, 2015.

Blair, S. L., MacMillan, A. C., Drozd, G. T., Goldstein, A. H., Chu, R. K., Pasa-Tolic, L., Shaw, J. B., Tolic, N., Lin, P., Laskin, J., Laskin, A., and Nizkorodov, S. A.: Molecular characterization of organosulfur compounds in biodiesel and biesel fuel secondary organic aerosol, Environ. Sci. Technol., 51, 119-127, doi: 10.1021/acs.est.6b03304, 2017.

Borbon, A., Fontaine, H., Veillerot, M., Locoge, N., Galloo, J. C., and Guillermo, R.: An investigation into the traffic-related fraction of isoprene at an urban location, Atmos. Environ., 35, 3749-3760, doi: 10.1016/S1352-2310(01)00170-4, 2001.

Brüggemann, M., Poulain, L., Held, A., Stelzer, T., Zuth, C., Richters, S., Mutzel, A., van Pinxteren, D., Iinuma, Y., Katkevica, S., Rabe, R., Herrmann, H., and Hoffmann, T.: Real-time detection of highly oxidized organosulfates and BSOA marker compounds during the F-BEACh 2014 field study, Atmos. Chem. Phys., 17, 1453-1469, doi: 10.5194/acp-17-1453-2017, 2017.

Bryant, D. J., Dixon, W. J., Hopkins, J. R., Dunmore, R. E., Pereira, K. L., Shaw, M., Squires, F. A., Bannan, T. J., Mehra, A., Worrall, S. D., Bacak, A., Coe, H., Percival, C. J., Whalley, L. K., Heard, D. E., Slater, E. J., Ouyang, B., Cui, T., Surratt, J. D., Liu, D., Shi, Z., Harrison, R., Sun, Y., Xu, W., Lewis, A. C., Lee, J. D., Rickard, A. R., and Hamilton, J. F.: Strong anthropogenic control of secondary organic aerosol formation from isoprene in Beijing, Atmos. Chem. Phys., 20, 7531-7552, doi: 10.5194/acp-20-7531-2020, 2020.

Budisulistiorini, S. H., Li, X., Bairai, S. T., Renfro, J., Liu, Y., Liu, Y. J., McKinney, K. A., Martin, S. T., McNeill, V. F., Pye, H. O. T., Nenes, A., Neff, M. E., Stone, E. A., Mueller, S., Knote, C., Shaw, S. L., Zhang, Z., Gold, A., and Surratt, J. D.: Examining the effects of anthropogenic emissions on isoprene-derived secondary organic aerosol formation during the 2013 Southern Oxidant and Aerosol Study (SOAS) at the Look Rock, Tennessee ground site, Atmos. Chem. Phys., 15, 8871-8888, doi: 10.5194/acp-15-8871-2015, 2015.

Chan, M. N., Surratt, J. D., Claeys, M., Edgerton, E. S., Tanner, R. L., Shaw, S. L., Zheng, M., Knipping, E. M., Eddingsaas, N. C., Wennberg, P. O., and Seinfeld, J. H.: Characterization and quantification of isoprene-derived epoxydiols in ambient aerosol in the southeastern United States, Environ. Sci. Technol., 44, 4590-4596, doi: 10.1021/es100596b, 2010.

Chan, M. N., Surratt, J. D., Chan, A. W. H., Schilling, K., Offenberg, J. H., Lewandowski, M., Edney, E. O., Kleindienst, T. E., Jaoui, M., Edgerton, E. S., Tanner, R. L., Shaw, S. L., Zheng, M., Knipping, E. M., and Seinfeld, J. H.: Influence of aerosol acidity on the chemical composition of secondary organic aerosol from β-caryophyllene, Atmos. Chem. Phys., 11, 1735-1751, doi: 10.5194/acp-11-1735-2011, 2011.

Chen, Y., Zhang, Y., Lambe, A. T., Xu, R., Lei, Z., Olson, N. E., Zhang, Z., Szalkowski, T., Cui, T., Vizuete, W., Gold, A., Turpin, B. J., Ault, A. P., Chan, M. N., and Surratt, J. D.: Heterogeneous hydroxyl radical oxidation of isoprene-epoxydiol-derived methyltetrol sulfates: plausible formation mechanisms of previously unexplained organosulfates in ambient fine aerosols, Environ. Sci. Technol. Lett., 7, 460-468, doi: 10.1021/acs.estlett.0c00276, 2020.

Claeys, M., Wang, W., Vermeylen, R., Kourtchev, I., Chi, X., Farhat, Y., Surratt, J. D., Gómez-González, Y., Sciare, J., and Maenhaut, W.: Chemical characterisation of marine aerosol at Amsterdam Island during the austral summer of 2006-2007, J. Aerosol Sci, 41, 13-22, doi: 10.1016/j.jaerosci.2009.08.003, 2010.

Darer, A. I., Cole-Filipiak, N. C., O'Connor, A. E., and Elrod, M. J.: Formation and stability of atmospherically relevant isoprene-derived organosulfates and organonitrates, Environ. Sci. Technol., 45, 1895-1902, doi: 10.1021/es103797z, 2011.

DeRieux, W.-S., Li, Y., Lin, P., Laskin, J., Laskin, A., Bertram, A. K., Nizkorodov, S. A., and Shiraiwa, M.: Predicting the glass transition temperature and viscosity of secondary organic material using molecular composition, Atmos. Chem. Phys., 18, 6331-6351, doi: 10.5194/acp-18-6331-2018, 2018.

Ding, A., Huang, X., Nie, W., Chi, X., Xu, Z., Zheng, L., Xu, Z., Xie, Y., Qi, X., Shen, Y., Sun, P., Wang, J., Wang, L., Sun, J., Yang, X.-Q., Qin, W., Zhang, X., Cheng, W., Liu, W., Pan, L., and Fu, C.: Significant reduction of PM2.5 in eastern China due to regional-scale emission control: evidence from SORPES in 2011-2018, Atmos. Chem. Phys., 19, 11791-11801, doi: 10.5194/acp-19-11791-2019, 2019a.

Ding, J., Zhao, P. S., Su, J., Dong, Q., Du, X., and Zhang, Y. F.: Aerosol pH and its driving factors in Beijing, Atmos. Chem. Phys., 19, 7939-7954, doi: 10.5194/acp-19-7939-2019, 2019b.

Estillore, A. D., Hettiyadura, A. P. S., Qin, Z., Leckrone, E., Wombacher, B., Humphry, T., Stone, E. A., and Grassian, V. H.: Water uptake and hygroscopic growth of organosulfate aerosol, Environ. Sci. Technol., 50, 4259-4268, doi: 10.1021/acs.est.5b05014, 2016.

Fisseha, R., Dommen, J., Gutzwiller, L., Weingartner, E., Gysel, M., Emmenegger, C., Kalberer, M., and Baltensperger, U.: Seasonal and diurnal characteristics of water soluble inorganic compounds in the gas and aerosol phase in the Zurich area, Atmos. Chem. Phys., 6, 1895-1904, doi: 10.5194/acp-6-1895-2006, 2006.

Fleming, L. T., Ali, N. N., Blair, S. L., Roveretto, M., George, C., and Nizkorodov, S. A.: Formation of light-absorbing organosulfates during evaporation of secondary organic material extracts in the presence of sulfuric acid, ACS Earth Space Chem., 3, 947-957, doi: 10.1021/acsearthspacechem.9b00036, 2019.

Fountoukis, C. and Nenes, A.: ISORROPIA II: a computationally efficient thermodynamic equilibrium model for K^+-Ca^{2+}-Mg^{2+}-NH_4^+-Na^+-SO_4^{2-}-NO_3^--Cl^--H_2O aerosols, Atmos. Chem. Phys., 7, 4639-4659, doi:10.5194/acp-7-4639-2007, 2007.

Froyd, K. D., Murphy, S. M., Murphy, D. M., de Gouw, J. A., Eddingsaas, N. C., and Wennberg, P. O.: Contribution of isoprene-derived organosulfates to free tropospheric aerosol mass, Proc. Natl. Acad. Sci. U.S.A., 107, 21360-21365, doi: 10.1073/pnas.1012561107, 2010.

https://doi.org/10.5194/acp-2020-784
Preprint. Discussion started: 14 September 2020

Atmospheric Chemistry and Physics Discussions

554 Gómez-González, Y., Surratt, J. D., Cuyckens, F., Szmigielski, R., Vermeylen, R., Jaoui, M., Lewandowski, M., Offenberg, J. H.,
555 Kleindienst, T. E., Edney, E. O., Blockhuys, F., Van Alsenoy, C., Maenhaut, W., and Claeys, M.: Characterization of
556 organosulfates from the photooxidation of isoprene and unsaturated fatty acids in ambient aerosol using liquid
557 chromatography/(-) electrospray ionization mass spectrometry, J. Mass Spectrom., 43, 371-382, doi: 10.1002/jms.1329, 2008.
558 Grgic, I., Dovzan, A., Bercic, G., and Hudnik, V.: The effect of atmospheric organic compounds on the Fe-catalyzed S(IV)
559 autoxidation in aqueous solution, J. Atmos. Chem., 29, 315-337, doi: 10.1023/a:1005918912994, 1998.
560 Griffith, S. M., Huang, X. H. H., Louie, P. K. K., and Yu, J. Z.: Characterizing the thermodynamic and chemical composition factors
561 controlling $PM_{2.5}$ nitrate: Insights gained from two years of online measurements in Hong Kong, Atmos. Environ., 122, 864-
562 875, doi: 10.1016/j.atmosenv.2015.02.009, 2015.
563 Guenther, A., Hewitt, C. N., Erickson, D., Fall, R., Geron, C., Graedel, T., Harley, P., Klinger, L., Lerdau, M., McKay, W. A., Pierce,
564 T., Scholes, B., Steinbrecher, R., Tallamraju, R., Taylor, J., and Zimmerman, P.: A global model of natural volatile organic
565 compound emissions, J. Geophys. Res., 100, 8873-8892, doi: 10.1029/94JD02950, 1995.
566 Guo, H., Xu, L., Bougiatioti, A., Cerully, K. M., Capps, S. L., Hite, J. R., Carlton, A. G., Lee, S. H., Bergin, M. H., Ng, N. L., Nenes,
567 A., and Weber, R. J.: Fine-particle water and pH in the southeastern United States, Atmos. Chem. Phys., 15, 5211-5228, doi:
568 10.5194/acp-15-5211-2015, 2015.
569 Guo, H., Sullivan, A. P., Campuzano-Jost, P., Schroder, J. C., Lopez-Hilfiker, F. D., Dibb, J. E., Jimenez, J. L., Thornton, J. A.,
570 Brown, S. S., Nenes, A., and Weber, R. J.: Fine particle pH and the partitioning of nitric acid during winter in the northeastern
571 United States, J. Geophys. Res. Atmos., 121, 10355-10376, doi: 10.1002/2016jd025311, 2016.
572 Hansen, A. M. K., Kristensen, K., Nguyen, Q. T., Zare, A., Cozzi, F., Nøjgaard, J. K., Skov, H., Brandt, J., Christensen, J. H., Ström,
573 J., Tunved, P., Krejci, R., and Glasius, M.: Organosulfates and organic acids in Arctic aerosols: speciation, annual variation and
574 concentration levels, Atmos. Chem. Phys., 14, 7807-7823, doi: 10.5194/acp-14-7807-2014, 2014.
575 Hansen, A. M. K., Hong, J., Raatikainen, T., Kristensen, K., Ylisirnio, A., Virtanen, A., Petaja, T., Glasius, M., and Prisle, N. L.:
576 Hygroscopic properties and cloud condensation nuclei activation of limonene-derived organosulfates and their mixtures with
577 ammonium sulfate, Atmos. Chem. Phys., 15, 14071-14089, doi: 10.5194/acp-15-14071-2015, 2015.
578 Hatch, L. E., Creamean, J. M., Ault, A. P., Surratt, J. D., Chan, M. N., Seinfeld, J. H., Edgerton, E. S., Su, Y., and Prather, K. A.:
579 Measurements of isoprene-derived organosulfates in ambient aerosols by aerosol time-of-flight mass spectrometry-part 2:
580 temporal variability and formation mechanisms, Environ. Sci. Technol., 45, 8648-8655, doi: 10.1021/es2011836, 2011.
581 Hawkins, L. N., Russell, L. M., Covert, D. S., Quinn, P. K., and Bates, T. S.: Carboxylic acids, sulfates, and organosulfates in
582 processed continental organic aerosol over the southeast Pacific Ocean during VOCALS-REx 2008, J. Geophys. Res., 115,
583 D13201, doi: 10.1029/2009jd013276, 2010.
584 He, Q. F., Ding, X., Wang, X. M., Yu, J. Z., Fu, X. X., Liu, T. Y., Zhang, Z., Xue, J., Chen, D. H., Zhong, L. J., and Donahue, N. M.:
585 Organosulfates from pinene and isoprene over the Pearl River Delta, South China: seasonal variation and implication in
586 formation mechanisms, Environ. Sci. Technol., 48, 9236-9245, doi: 10.1021/es501299v, 2014.
587 He, Q. F., Ding, X., Fu, X. X., Zhang, Y. Q., Wang, J. Q., Liu, Y. X., Tang, M. J., Wang, X. M., and Rudich, Y.: Secondary organic
588 aerosol formation from isoprene epoxides in the Pearl River Delta, south China: IEPOX- and HMML-derived tracers, J. Geophys.
589 Res.-Atmos., 123, 6999-7012, doi: 10.1029/2017jd028242, 2018.
590 Hennigan, C. J., Izumi, J., Sullivan, A. P., Weber, R. J., and Nenes, A.: A critical evaluation of proxy methods used to estimate the
591 acidity of atmospheric particles, Atmos. Chem. Phys., 15, 2775-2790, doi: 10.5194/acp-15-2775-2015, 2015.
592 Herrmann, H.: Kinetics of aqueous phase reactions relevant for atmospheric chemistry, Chem. Rev., 103, 4691-4716, doi:
593 10.1021/cr020658q, 2003.
594 Hettiyadura, A. P. S., Stone, E. A., Kundu, S., Baker, Z., Geddes, E., Richards, K., and Humphry, T.: Determination of atmospheric
595 organosulfates using HILIC chromatography with MS detection, Atmos. Meas. Tech., 8, 2347-2358, doi: 10.5194/amt-8-2347-
596 2015, 2015.
597 Hettiyadura, A. P. S., Jayarathne, T., Baumann, K., Goldstein, A. H., de Gouw, J. A., Koss, A., Keutsch, F. N., Skog, K., and Stone,
598 E. A.: Qualitative and quantitative analysis of atmospheric organosulfates in Centreville, Alabama, Atmos. Chem. Phys., 17,
599 1343-1359, doi: 10.5194/acp-17-1343-2017, 2017.
600 Hettiyadura, A. P. S., Al-Naiema, I. M., Hughes, D. D., Fang, T., and Stone, E. A.: Organosulfates in Atlanta, Georgia: anthropogenic
601 influences on biogenic secondary organic aerosol formation, Atmos. Chem. Phys., 19, 3191-3206, doi: 10.5194/acp-19-3191-
602 2019, 2019.
603 Hoffmann, T., Huang, R. J., and Kalberer, M.: Atmospheric analytical chemistry, Anal. Chem., 83, 4649-4664, doi:
604 10.1021/ac2010718, 2011.
605 Huang, L., Coddens, E. M., and Grassian, V. H.: Formation of organosulfur compounds from aqueous phase reactions of S(IV) with
606 methacrolein and methyl vinyl ketone in the presence of transition metal ions, ACS Earth Space Chem., 3, 1749-1755, doi:
607 10.1021/acsearthspacechem.9b00173, 2019.
608 Huang, R.-J., Zhang, Y., Bozzetti, C., Ho, K.-F., Cao, J.-J., Han, Y., Daellenbach, K. R., Slowik, J. G., Platt, S. M., Canonaco, F.,
609 Zotter, P., Wolf, R., Pieber, S. M., Bruns, E. A., Crippa, M., Ciarelli, G., Piazzalunga, A., Schwikowski, M., Abbaszade, G.,
610 Schnelle-Kreis, J., Zimmermann, R., An, Z., Szidat, S., Baltensperger, U., El Haddad, I., and Prevot, A. S. H.: High secondary
611 aerosol contribution to particulate pollution during haze events in China, Nature, 514, 218-222, doi: 10.1038/nature13774, 2014.
612 Huang, R.-J., Cao, J., Chen, Y., Yang, L., Shen, J., You, Q., Wang, K., Lin, C., Xu, W., Gao, B., Li, Y., Chen, Q., Hoffmann, T., amp,
613 apos, Dowd, C. D., Bilde, M., and Glasius, M.: Organosulfates in atmospheric aerosol: synthesis and quantitative analysis of
614 PM2.5 from Xi'an, northwestern China, Atmos. Meas. Tech., 11, 3447-3456, doi: 10.5194/amt-11-3447-2018, 2018.
615 Iinuma, Y., Mueller, C., Berndt, T., Boege, O., Claeys, M., and Herrmann, H.: Evidence for the existence of organosulfates from β-

https://doi.org/10.5194/acp-2020-784
Preprint. Discussion started: 14 September 2020

Atmospheric Chemistry and Physics Discussions

pinene ozonolysis in ambient secondary organic aerosol, Environ. Sci. Technol., 41, 6678-6683, doi: 10.1021/es070938t, 2007a.
Iinuma, Y., Mueller, C., Boege, O., Gnauk, T., and Herrmann, H.: The formation of organic sulfate esters in the limonene ozonolysis secondary organic aerosol (SOA) under acidic conditions, Atmos. Environ., 41, 5571-5583, doi: 10.1016/j.atmosenv.2007.03.007, 2007b.
Iinuma, Y., Boege, O., Kahnt, A., and Herrmann, H.: Laboratory chamber studies on the formation of organosulfates from reactive uptake of monoterpene oxides, Phys. Chem. Chem. Phys., 11, 7985-7997, doi: 10.1039/b904025k, 2009.
Jiang, P.-Y., Katsumura, Y., Domae, M., Ishikawa, K., Ishigure, K., and Yoshida, Y.: Pulse radiolysis study of concentrated sulfuric acid solutions. Formation mechanism, yield and reactivity of sulfate radicals, J. Chem. Soc., Faraday Trans., 88, 3319-3222, doi: 10.1039/ft9928801653, 1992.
Jimenez, J. L., Canagaratna, M. R., Donahue, N. M., Prevot, A. S. H., Zhang, Q., Kroll, J. H., DeCarlo, P. F., Allan, J. D., Coe, H., Ng, N. L., Aiken, A. C., Docherty, K. S., Ulbrich, I. M., Grieshop, A. P., Robinson, A. L., Duplissy, J., Smith, J. D., Wilson, K. R., Lanz, V. A., Hueglin, C., Sun, Y. L., Tian, J., Laaksonen, A., Raatikainen, T., Rautiainen, J., Vaattovaara, P., Ehn, M., Kulmala, M., Tomlinson, J. M., Collins, D. R., Cubison, M. J., Dunlea, E. J., Huffman, J. A., Onasch, T. B., Alfarra, M. R., Williams, P. I., Bower, K., Kondo, Y., Schneider, J., Drewnick, F., Borrmann, S., Weimer, S., Demerjian, K., Salcedo, D., Cottrell, L., Griffin, R., Takami, A., Miyoshi, T., Hatakeyama, S., Shimono, A., Sun, J. Y., Zhang, Y. M., Dzepina, K., Kimmel, J. R., Sueper, D., Jayne, J. T., Herndon, S. C., Trimborn, A. M., Williams, L. R., Wood, E. C., Middlebrook, A. M., Kolb, C. E., Baltensperger, U., and Worsnop, D. R.: Evolution of organic aerosols in the atmosphere, Science, 326, 1525-1529, doi: 10.1126/science.1180353, 2009.
Johnston, M. V. and Kerecman, D. E.: Molecular characterization of atmospheric organic aerosol by mass spectrometry, Annu. Rev. Anal. Chem., 12, 247-274, doi: 10.1146/annurev-anchem-061516-045135, 2019.
Kourtchev, I., Godoi, R. H. M., Connors, S., Levine, J. G., Archibald, A. T., Godoi, A. F. L., Paralovo, S. L., Barbosa, C. G. G., Souza, R. A. F., Manzi, A. O., Seco, R., Sjostedt, S., Park, J.-H., Guenther, A., Kim, S., Smith, J., Martin, S. T., and Kalberer, M.: Molecular composition of organic aerosols in central Amazonia: an ultra-high-resolution mass spectrometry study, Atmos. Chem. Phys., 16, 11899-11913, doi: 10.5194/acp-16-11899-2016, 2016.
Kristensen, K. and Glasius, M.: Organosulfates and oxidation products from biogenic hydrocarbons in fine aerosols from a forest in North West Europe during spring, Atmos. Environ., 45, 4546-4556, doi: 10.1016/j.atmosenv.2011.05.063, 2011.
Kundu, S., Quraishi, T. A., Yu, G., Suarez, C., Keutsch, F. N., and Stone, E. A.: Evidence and quantitation of aromatic organosulfates in ambient aerosols in Lahore, Pakistan, Atmos. Chem. Phys., 13, 4865-4875, doi: 10.5194/acp-13-4865-2013, 2013.
Le Breton, M., Wang, Y., Hallquist, Å. M., Pathak, R. K., Zheng, J., Yang, Y., Shang, D., Glasius, M., Bannan, T. J., Liu, Q., Chan, C. K., Percival, C. J., Zhu, W., Lou, S., Topping, D., Wang, Y., Yu, J., Lu, K., Guo, S., Hu, M., and Hallquist, M.: Online gas- and particle-phase measurements of organosulfates, organosulfonates and nitrooxy organosulfates in Beijing utilizing a FIGAERO ToF-CIMS, Atmos. Chem. Phys., 18, 10355-10371, doi: 10.5194/acp-18-10355-2018, 2018.
Lewandowski, M., Jaoui, M., Offenberg, J. H., Krug, J. D., and Kleindienst, T. E.: Atmospheric oxidation of isoprene and 1,3-butadiene: influence of aerosol acidity and relative humidity on secondary organic aerosol, Atmos. Chem. Phys., 15, 3773-3783, doi: 10.5194/acp-15-3773-2015, 2015.
Liao, J., Froyd, K. D., Murphy, D. M., Keutsch, F. N., Yu, G., Wennberg, P. O., St. Clair, J. M., Crounse, J. D., Wisthaler, A., Mikoviny, T., Jimenez, J. L., Campuzano-Jost, P., Day, D. A., Hu, W., Ryerson, T. B., Pollack, I. B., Peischl, J., Anderson, B. E., Ziemba, L. D., Blake, D. R., Meinardi, S., and Diskin, G.: Airborne measurements of organosulfates over the continental US, J. Geophys. Res. Atmos., 120, 2990-3005, doi: 10.1002/2014jd022378, 2015.
Lin, P., Yu, J. Z., Engling, G., and Kalberer, M.: Organosulfates in humic-like substance fraction isolated from aerosols at seven locations in East Asia: a study by ultra-high-resolution mass spectrometry, Environ. Sci. Technol., 46, 13118-13127, doi: 10.1021/es303570v, 2012a.
Lin, Y. H., Zhang, Z., Docherty, K. S., Zhang, H., Budisulistiorini, S. H., Rubitschun, C. L., Shaw, S. L., Knipping, E. M., Edgerton, E. S., Kleindienst, T. E., Gold, A., and Surratt, J. D.: Isoprene epoxydiols as precursors to secondary organic aerosol formation: acid-catalyzed reactive uptake studies with authentic compounds, Environ. Sci. Technol., 46, 250-258, doi: 10.1021/es202554c, 2012b.
Lin, Y. H., Zhang, H., Pye, H. O., Zhang, Z., Marth, W. J., Park, S., Arashiro, M., Cui, T., Budisulistiorini, S. H., Sexton, K. G., Vizuete, W., Xie, Y., Luecken, D. J., Piletic, I. R., Edney, E. O., Bartolotti, L. J., Gold, A., and Surratt, J. D.: Epoxide as a precursor to secondary organic aerosol formation from isoprene photooxidation in the presence of nitrogen oxides, Proc. Natl. Acad. Sci. U.S.A., 110, 6718-6723, doi: 10.1073/pnas.1221150110, 2013.
Liu, M. X., Song, Y., Zhou, T., Xu, Z. Y., Yan, C. Q., Zheng, M., Wu, Z. J., Hu, M., Wu, Y. S., and Zhu, T.: Fine particle pH during severe haze episodes in northern China, Geophys. Res. Lett., 44, 5213-5221, doi: 10.1002/2017gl073210, 2017.
Liu, Y. and Wang, T.: Worsening urban ozone pollution in China from 2013 to 2017-Part 2: The effects of emission changes and implications for multi-pollutant control, Atmos. Chem. Phys., 20, 6323-6337, doi: 10.5194/acp-20-6323-2020, 2020.
Lukacs, H., Gelencser, A., Hoffer, A., Kiss, G., Horvath, K., and Hartyani, Z.: Quantitative assessment of organosulfates in size-segregated rural fine aerosol, Atmos. Chem. Phys., 9, 231-238, doi: 10.5194/acp-9-231-2009, 2009.
Ma, Y., Xu, X., Song, W., Geng, F., and Wang, L.: Seasonal and diurnal variations of particulate organosulfates in urban Shanghai, China, Atmos. Environ., 85, 152-160, doi: 10.1016/j.atmosenv.2013.12.017, 2014.
Mahowald, N.: Aerosol indirect effect on biogeochemical cycles and climate, Science, 334, 794-796, doi: 10.1126/science.1207374, 2011.
McNeill, V. F., Woo, J. L., Kim, D. D., Schwier, A. N., Wannell, N. J., Sumner, A. J., and Barakat, J. M.: Aqueous-phase secondary organic aerosol and organosulfate formation in atmospheric aerosols: a modeling study, Environ. Sci. Technol., 46, 8075-8081,

https://doi.org/10.5194/acp-2020-784
Preprint. Discussion started: 14 September 2020

Atmospheric Chemistry and Physics Discussions

678 doi: 10.1021/es3002986, 2012.
679 Meade, L. E., Riva, M., Blomberg, M. Z., Brock, A. K., Qualters, E. M., Siejack, R. A., Ramakrishnan, K., Surratt, J. D., and
680 Kautzman, K. E.: Seasonal variations of fine particulate organosulfates derived from biogenic and anthropogenic hydrocarbons
681 in the mid-Atlantic United States, Atmos. Environ., 145, 405-414, doi: 10.1016/j.atmosenv.2016.09.028, 2016.
682 Nah, T., Guo, H. Y., Sullivan, A. P., Chen, Y. L., Tanner, D. J., Nenes, A., Russell, A., Ng, N. L., Huey, L. G., and Weber, R. J.:
683 Characterization of aerosol composition, aerosol acidity, and organic acid partitioning at an agriculturally intensive rural
684 southeastern US site, Atmos. Chem. Phys., 18, 11471-11491, doi: 10.5194/acp-18-11471-2018, 2018.
685 Nestorowicz, K., Jaoui, M., Rudzinski, K. J., Lewandowski, M., Kleindienst, T. E., Spolnik, G., Danikiewicz, W., and Szmigielski,
686 R.: Chemical composition of isoprene SOA under acidic and non-acidic conditions: effect of relative humidity, Atmos. Chem.
687 Phys., 18, 18101-18121, doi: 10.5194/acp-18-18101-2018, 2018.
688 Nguyen, Q. T., Christensen, M. K., Cozzi, F., Zare, A., Hansen, A. M. K., Kristensen, K., Tulinius, T. E., Madsen, H. H., Christensen,
689 J. H., Brandt, J., Massling, A., Nøjgaard, J. K., and Glasius, M.: Understanding the anthropogenic influence on formation of
690 biogenic secondary organic aerosols in Denmark via analysis of organosulfates and related oxidation products, Atmos. Chem.
691 Phys., 14, 8961-8981, doi: 10.5194/acp-14-8961-2014, 2014.
692 Nguyen, T. B., Lee, P. B., Updyke, K. M., Bones, D. L., Laskin, J., Laskin, A., and Nizkorodov, S. A.: Formation of nitrogen- and
693 sulfur-containing light-absorbing compounds accelerated by evaporation of water from secondary organic aerosols, J. Geophys.
694 Res.-Atmos., 117, D01207, doi: 10.1029/2011jd016944, 2012.
695 Nguyen, T. B., Bates, K. H., Crounse, J. D., Schwantes, R. H., Zhang, X., Kjaergaard, H. G., Surratt, J. D., Lin, P., Laskin, A.,
696 Seinfeld, J. H., and Wennberg, P. O.: Mechanism of the hydroxyl radical oxidation of methacryloyl peroxynitrate (MPAN) and
697 its pathway toward secondary organic aerosol formation in the atmosphere, Phys. Chem. Chem. Phys., 17, 17914-17926, doi:
698 10.1039/c5cp02001h, 2015.
699 Nozière, B., Ekström, S., Alsberg, T., and Holmström, S.: Radical-initiated formation of organosulfates and surfactants in
700 atmospheric aerosols, Geophys. Res. Lett., 37, L05806, doi: 10.1029/2009gl041683, 2010.
701 Nozière, B., Kalberer, M., Claeys, M., Allan, J., D'Anna, B., Decesari, S., Finessi, E., Glasius, M., Grgic, I., Hamilton, J. F.,
702 Hoffmann, T., Iinuma, Y., Jaoui, M., Kahno, A., Kampf, C. J., Kourtchev, I., Maenhaut, W., Marsden, N., Saarikoski, S.,
703 Schnelle-Kreis, J., Surratt, J. D., Szidat, S., Szmigielski, R., and Wisthaler, A.: The molecular identification of organic
704 compounds in the atmosphere: state of the art and challenges, Chem. Rev., 115, 3919-3983, doi: 10.1021/cr5003485, 2015.
705 Olson, C. N., Galloway, M. M., Yu, G., Hedman, C. J., Lockett, M. R., Yoon, T., Stone, E. A., Smith, L. M., and Keutsch, F. N.:
706 Hydroxycarboxylic acid-derived organosulfates: synthesis, stability, and quantification in ambient aerosol, Environ. Sci.
707 Technol., 45, 6468-6474, doi: 10.1021/es201039p, 2011.
708 Olson, N. E., Lei, Z. Y., Craig, R. L., Zhang, Y., Chen, Y. Z., Lambe, A. T., Zhang, Z. F., Gold, A., Surratt, J. D., and Ault, A. P.:
709 Reactive uptake of isoprene epoxydiols increases the viscosity of the core of phase-separated aerosol particles, ACS Earth Space
710 Chem., 3, 1402-1414, doi: 10.1021/acsearthspacechem.9b00138, 2019.
711 Passananti, M., Kong, L., Shang, J., Dupart, Y., Perrier, S., Chen, J., Donaldson, D. J., and George, C.: Organosulfate formation
712 through the heterogeneous reaction of sulfur dioxide with unsaturated fatty acids and long-chain alkenes, Angew. Chem. Int.
713 Ed., 55, 10336-10339, doi: 10.1002/anie.201605266, 2016.
714 Pye, H. O. T., Pinder, R. W., Piletic, I. R., Xie, Y., Capps, S. L., Lin, Y. H., Surratt, J. D., Zhang, Z. F., Gold, A., Luecken, D. J.,
715 Hutzell, W. T., Jaoui, M., Offenberg, J. H., Kleindienst, T. E., Lewandowski, M., and Edney, E. O.: Epoxide pathways improve
716 model predictions of isoprene markers and reveal key role of acidity in aerosol formation, Environ. Sci. Technol., 47, 11056-
717 11064, doi: 10.1021/es402106h, 2013.
718 Ramanathan, V., Crutzen, P. J., Lelieveld, J., Mitra, A. P., Althausen, D., Anderson, J., Andreae, M. O., Cantrell, W., Cass, G. R.,
719 Chung, C. E., Clarke, A. D., Coakley, J. A., Collins, W. D., Conant, W. C., Dulac, F., Heintzenberg, J., Heymsfield, A. J., Holben,
720 B., Howell, S., Hudson, J., Jayaraman, A., Kiehl, J. T., Krishnamurti, T. N., Lubin, D., McFarquhar, G., Novakov, T., Ogren, J.
721 A., Podgorny, I. A., Prather, K., Priestley, K., Prospero, J. M., Quinn, P. K., Rajeev, K., Rasch, P., Rupert, S., Sadourny, R.,
722 Satheesh, S. K., Shaw, G. E., Sheridan, P., and Valero, F. P. J.: Indian Ocean Experiment: an integrated analysis of the climate
723 forcing and effects of the great Indo-Asian haze, J. Geophys. Res. Atmos., 106, 28371-28398, doi: 10.1029/2001jd900133, 2001.
724 Rattanavaraha, W., Chu, K., Budisulistiorini, S. H., Riva, M., Lin, Y. H., Edgerton, E. S., Baumann, K., Shaw, S. L., Guo, H., King,
725 L., Weber, R. J., Neff, M. E., Stone, E. A., Offenberg, J. H., Zhang, Z., Gold, A., and Surratt, J. D.: Assessing the impact of
726 anthropogenic pollution on isoprene-derived secondary organic aerosol formation in $PM_{2.5}$ collected from the Birmingham,
727 Alabama, ground site during the 2013 Southern Oxidant and Aerosol Study, Atmos. Chem. Phys., 16, 4897-4914, doi:
728 10.5194/acp-16-4897-2016, 2017.
729 Riva, M., Tomaz, S., Cui, T., Lin, Y. H., Perraudin, E., Gold, A., Stone, E. A., Villenave, E., and Surratt, J. D.: Evidence for an
730 unrecognized secondary anthropogenic source of organosulfates and sulfonates: gas-phase oxidation of polycyclic aromatic
731 hydrocarbons in the presence of sulfate aerosol, Environ. Sci. Technol., 49, 6654-6664, doi: 10.1021/acs.est.5b00836, 2015.
732 Riva, M., Budisulistiorini, S. H., Zhang, Z. F., Gold, A., and Surratt, J. D.: Chemical characterization of secondary organic aerosol
733 constituents from isoprene ozonolysis in the presence of acidic aerosol, Atmos. Environ., 130, 5-13, doi:
734 10.1016/j.atmosenv.2015.06.027, 2016a.
735 Riva, M., Da Silva Barbosa, T., Lin, Y.-H., Stone, E. A., Gold, A., and Surratt, J. D.: Chemical characterization of organosulfates in
736 secondary organic aerosol derived from the photooxidation of alkanes, Atmos. Chem. Phys., 16, 11001-11018, doi: 10.5194/acp-
737 16-11001-2016, 2016b.
738 Riva, M., Chen, Y., Zhang, Y., Lei, Z., Olson, N. E., Boyer, H. C., Narayan, S., Yee, L. D., Green, H. S., Cui, T., Zhang, Z., Baumann,
739 K., Fort, M., Edgerton, E., Budisulistiorini, S. H., Rose, C. A., Ribeiro, I. O., RL, E. O., Dos Santos, E. O., Machado, C. M. D.,

https://doi.org/10.5194/acp-2020-784
Preprint. Discussion started: 14 September 2020

Atmospheric Chemistry and Physics Discussions

740 Szopa, S., Zhao, Y., Alves, E. G., de Sa, S. S., Hu, W., Knipping, E. M., Shaw, S. L., Duvoisin Junior, S., de Souza, R. A. F.,
741 Palm, B. B., Jimenez, J. L., Glasius, M., Goldstein, A. H., Pye, H. O. T., Gold, A., Turpin, B. J., Vizuete, W., Martin, S. T.,
742 Thornton, J. A., Dutcher, C. S., Ault, A. P., and Surratt, J. D.: Increasing isoprene epoxydiol-to-inorganic sulfate aerosol ratio
743 results in extensive conversion of inorganic sulfate to organosulfur forms: implications for aerosol physicochemical properties,
744 Environ. Sci. Technol., 53, 8682-8694, doi: 10.1021/acs.est.9b01019, 2019.
745 Schindelka, J., Iinuma, Y., Hoffmann, D., and Herrmann, H.: Sulfate radical-initiated formation of isoprene-derived organosulfates
746 in atmospheric aerosols, Faraday Discuss., 165, 237-259, doi: 10.1039/c3fd00042g, 2013.
747 Shakya, K. M. and Peltier, R. E.: Investigating missing sources of sulfur at Fairbanks, Alaska, Environ. Sci. Technol., 47, 9332-
748 9338, doi: 10.1021/es402020b, 2013.
749 Shakya, K. M. and Peltier, R. E.: Non-sulfate sulfur in fine aerosols across the United States: Insight for organosulfate prevalence,
750 Atmospheric Environment, 100, 159-166, doi: 10.1016/j.atmosenv.2014.10.058, 2015.
751 Shalamzari, M. S., Ryabtsova, O., Kahnt, A., Vermeylen, R., Herent, M. F., Quetin-Leclercq, J., Van der Veken, P., Maenhaut, W.,
752 and Claeys, M.: Mass spectrometric characterization of organosulfates related to secondary organic aerosol from isoprene, Rapid
753 Commun. Mass Spectrom., 27, 784-794, doi: 10.1002/rcm.6511, 2013.
754 Shang, J., Passananti, M., Dupart, Y., Ciuraru, R., Tinel, L., Rossignol, S., Perrier, S., Zhu, T., and George, C.: SO_2 uptake on oleic
755 acid: a new formation pathway of organosulfur compounds in the atmosphere, Environ. Sci. Technol. Lett., 3, 67-72, doi:
756 10.1021/acs.estlett.6b00006, 2016.
757 Shi, G. L., Xu, J., Peng, X., Xiao, Z. M., Chen, K., Tian, Y. Z., Guan, X. B., Feng, Y. C., Yu, H. F., Nenes, A., and Russell, A. G.:
758 pH of aerosols in a polluted atmosphere: source contributions to highly acidic aerosol, Environ. Sci. Technol., 51, 4289-4296,
759 doi: 10.1021/acs.est.6b05736, 2017.
760 Shiraiwa, M., Ammann, M., Koop, T., and Poschl, U.: Gas uptake and chemical aging of semisolid organic aerosol particles, Proc.
761 Natl. Acad. Sci. U.S.A., 108, 11003-11008, doi: 10.1073/pnas.1103045108, 2011.
762 Shrivastava, M., Cappa, C. D., Fan, J. W., Goldstein, A. H., Guenther, A. B., Jimenez, J. L., Kuang, C., Laskin, A., Martin, S. T.,
763 Ng, N. L., Petaja, T., Pierce, J. R., Rasch, P. J., Roldin, P., Seinfeld, J. H., Shilling, J., Smith, J. N., Thornton, J. A., Volkamer,
764 R., Wang, J., Worsnop, D. R., Zaveri, R. A., Zelenyuk, A., and Zhang, Q.: Recent advances in understanding secondary organic
765 aerosol: Implications for global climate forcing, Rev. Geophys., 55, 509-559, doi: 10.1002/2016RG000540, 2017.
766 Song, S., Nenes, A., Gao, M., Zhang, Y., Liu, P., Shao, J., Ye, D., Xu, W., Lei, L., Sun, Y., Liu, B., Wang, S., and McElroy, M. B.:
767 Thermodynamic modeling suggests declines in water uptake and acidity of inorganic aerosols in Beijing winter haze events
768 during 2014/2015-2018/2019, Environ. Sci. Technol. Lett., 6, 752-760, doi: 10.1021/acs.estlett.9b00621, 2019.
769 Staudt, S., Kundu, S., Lehmler, H. J., He, X., Cui, T., Lin, Y. H., Kristensen, K., Glasius, M., Zhang, X., Weber, R. J., Surratt, J. D.,
770 and Stone, E. A.: Aromatic organosulfates in atmospheric aerosols: synthesis, characterization, and abundance, Atmos. Environ.,
771 94, 366-373, doi: 10.1016/j.atmosenv.2014.05.049, 2014.
772 Stone, E. A., Yang, L., Yu, L. E., and Rupakheti, M.: Characterization of organosulfates in atmospheric aerosols at Four Asian
773 locations, Atmos. Environ., 47, 323-329, doi: 10.1016/j.atmosenv.2011.10.058, 2012.
774 Surratt, J. D., Kroll, J. H., Kleindienst, T. E., Edney, E. O., Claeys, M., Sorooshian, A., Ng, N. L., Offenberg, J. H., Lewandowski,
775 M., Jaoui, M., Flagan, R. C., and Seinfeld, J. H.: Evidence for organosulfates in secondary organic aerosol, Environ. Sci. Technol.,
776 41, 517-527, doi: 10.1021/es062081q, 2007a.
777 Surratt, J. D., Lewandowski, M., Offenberg, J. H., Jaoui, M., Kleindienst, T. E., Edney, E. O., and Seinfeld, J. H.: Effect of acidity
778 on secondary organic aerosol formation from isoprene, Environ. Sci. Technol., 41, 5363-5369, doi: 10.1021/es0704176, 2007b.
779 Surratt, J. D., Gómez-González, Y., Chan, A. W. H., Vermeylen, R., Shahgholi, M., Kleindienst, T. E., Edney, E. O., Offenberg, J.
780 H., Lewandowski, M., Jaoui, M., Maenhaut, W., Claeys, M., Richard C. Flagan, and Seinfeld, J. H.: Organosulfate formation in
781 biogenic secondary organic aerosol, J. Phys. Chem. A, 8345–8378, doi: 10.1021/jp802310p, 2008.
782 Surratt, J. D., Chan, A. W., Eddingsaas, N. C., Chan, M., Loza, C. L., Kwan, A. J., Hersey, S. P., Flagan, R. C., Wennberg, P. O., and
783 Seinfeld, J. H.: Reactive intermediates revealed in secondary organic aerosol formation from isoprene, Proc. Natl. Acad. Sci.
784 U.S.A., 107, 6640-6645, doi: 10.1073/pnas.0911114107, 2010.
785 Tao, J., Zhang, L., Cao, J., and Zhang, R.: A review of current knowledge concerning $PM_{2.5}$ chemical composition, aerosol optical
786 properties and their relationships across China, Atmos. Chem. Phys., 17, 9485-9518, doi: 10.5194/acp-17-9485-2017, 2017.
787 Tao, S., Lu, X., Levac, N., Bateman, A. P., Nguyen, T. B., Bones, D. L., Nizkorodov, S. A., Laskin, J., Laskin, A., and Yang, X.:
788 Molecular characterization of organosulfates in organic aerosols from Shanghai and Los Angeles urban areas by nanospray-
789 desorption electrospray ionization high-resolution mass spectrometry, Environ. Sci. Technol., 48, 10993-11001, doi:
790 10.1021/es5024674, 2014.
791 Tolocka, M. P. and Turpin, B.: Contribution of organosulfur compounds to organic aerosol mass, Environ. Sci. Technol., 46, 7978-
792 7983, doi: 10.1021/es300651v, 2012.
793 Wach, P., Spolnik, G., Rudzinski, K. J., Skotak, K., Claeys, M., Danikiewicz, W., and Szmigielski, R.: Radical oxidation of methyl
794 vinyl ketone and methacrolein in aqueous droplets: Characterization of organosulfates and atmospheric implications,
795 Chemosphere, 214, 1-9, doi: 10.1016/j.chemosphere.2018.09.026, 2019.
796 Wang, H. C., Chen, X. R., Lu, K. D., Hu, R. Z., Li, Z. Y., Wang, H. L., Ma, X. F., Yang, X. P., Chen, S. Y., Dong, H. B., Liu, Y.,
797 Fang, X., Zeng, L. M., Hu, M., and Zhang, Y. H.: NO_3 and N_2O_5 chemistry at a suburban site during the EXPLORE-YRD
798 campaign in 2018, Atmos. Environ., 224, 117180, doi: 10.1016/j.atmosenv.2019., 2020a.
799 Wang, H. L., Qiao, L. P., Lou, S. R., Zhou, M., Ding, A. J., Huang, H. Y., Chen, J. M., Wang, Q., Tao, S. K., Chen, C. H., Li, L., and
800 Huang, C.: Chemical composition of $PM_{2.5}$ and meteorological impact among three years in urban Shanghai, China, J. Clean.
801 Prod., 112, 1302-1311, doi: 10.1016/j.jclepro.2015.04.099, 2016a.

https://doi.org/10.5194/acp-2020-784
Preprint. Discussion started: 14 September 2020

Atmospheric Chemistry and Physics Discussions

802 Wang, J. J., Lu, X. M., Yan, Y. T., Zhou, L. G., and Ma, W. C.: Spatiotemporal characteristics of $PM_{2.5}$ concentration in the Yangtze
803 River Delta urban agglomeration, China on the application of big data and wavelet analysis, Sci. Total Environ., 724, 138134,
804 doi: 10.1016/j.scitotenv.2020., 2020b.
805 Wang, K., Zhang, Y., Huang, R. J., Wang, M., Ni, H., Kampf, C. J., Cheng, Y., Bilde, M., Glasius, M., and Hoffmann, T.: Molecular
806 characterization and source identification of atmospheric particulate organosulfates using ultrahigh resolution mass spectrometry,
807 Environ. Sci. Technol., 53, 6192-6202, doi: 10.1021/acs.est.9b02628, 2019a.
808 Wang, S. Y., Zhou, S. M., Tao, Y., Tsui, W. G., Ye, J. H., Yu, J. Z., Murphy, J. G., McNeill, V. F., Abbatt, J. P. D., and Chan, A. W.
809 H.: Organic peroxides and sulfur dioxide in aerosol: source of particulate sulfate, Environ. Sci. Technol., 53, 10695-10704, doi:
810 10.1021/acs.est.9b02591, 2019b.
811 Wang, X. K., Rossignol, S., Ma, Y., Yao, L., Wang, M. Y., Chen, J. M., George, C., and Wang, L.: Molecular characterization of
812 atmospheric particulate organosulfates in three megacities at the middle and lower reaches of the Yangtze River, Atmos. Chem.
813 Phys., 16, 2285-2298, doi: 10.5194/acp-16-2285-2016, 2016b.
814 Wang, Y., Ren, J., Huang, X. H. H., Tong, R., and Yu, J. Z.: Synthesis of four monoterpene-derived organosulfates and their
815 quantification in atmospheric aerosol samples, Environ. Sci. Technol., 51, 6791-6801, doi: 10.1021/acs.est.7b01179, 2017.
816 Wang, Y., Hu, M., Guo, S., Wang, Y., Zheng, J., Yang, Y., Zhu, W., Tang, R., Li, X., Liu, Y., Le Breton, M., Du, Z., Shang, D., Wu,
817 Y., Wu, Z., Song, Y., Lou, S., Hallquist, M., and Yu, J.: The secondary formation of organosulfates under interactions between
818 biogenic emissions and anthropogenic pollutants in summer in Beijing, Atmos. Chem. Phys., 18, 10693-10713, doi:
819 10.5194/acp-18-10693-2018, 2018.
820 Wen, L., Xue, L. K., Wang, X. F., Xu, C. H., Chen, T. S., Yang, L. X., Wang, T., Zhang, Q. Z., and Wang, W. X.: Summertime fine
821 particulate nitrate pollution in the North China Plain: increasing trends, formation mechanisms and implications for control
822 policy, Atmos. Chem. Phys., 18, 11261-11275, doi: 10.5194/acp-18-11261-2018, 2018.
823 Worton, D. R., Surratt, J. D., Lafranchi, B. W., Chan, A. W., Zhao, Y., Weber, R. J., Park, J. H., Gilman, J. B., de Gouw, J., Park, C.,
824 Schade, G., Beaver, M., Clair, J. M., Crounse, J., Wennberg, P., Wolfe, G. M., Harrold, S., Thornton, J. A., Farmer, D. K.,
825 Docherty, K. S., Cubison, M. J., Jimenez, J. L., Frossard, A. A., Russell, L. M., Kristensen, K., Glasius, M., Mao, J., Ren, X.,
826 Brune, W., Browne, E. C., Pusede, S. E., Cohen, R. C., Seinfeld, J. H., and Goldstein, A. H.: Observational insights into aerosol
827 formation from isoprene, Environ. Sci. Technol., 47, 11403-11413, doi: 10.1021/es4011064, 2013.
828 Yao, M., Zhao, Y., Hu, M., Huang, D., Wang, Y., Yu, J. Z., and Yan, N.: Multiphase reactions between secondary organic aerosol
829 and sulfur dioxide: kinetics and contributions to sulfate formation and aerosol aging, Environ. Sci. Technol. Lett., 6, 768-774,
830 doi: 10.1021/acs.estlett.9b00657, 2019.
831 Yassine, M. M., Dabek-Zlotorzynska, E., Harir, M., and Schmitt-Kopplin, P.: Identification of weak and strong organic acids in
832 atmospheric aerosols by capillary electrophoresis/mass spectrometry and ultra-high-resolution fourier transform ion cyclotron
833 resonance mass spectrometry, Anal. Chem., 84, 6586-6594, doi: 10.1021/ac300798g, 2012.
834 Zhang, H., Worton, D. R., Lewandowski, M., Ortega, J., Rubitschun, C. L., Park, J. H., Kristensen, K., Campuzano-Jost, P., Day, D.
835 A., Jimenez, J. L., Jaoui, M., Offenberg, J. H., Kleindienst, T. E., Gilman, J., Kuster, W. C., de Gouw, J., Park, C., Schade, G.
836 W., Frossard, A. A., Russell, L., Kaser, L., Jud, W., Hansel, A., Cappellin, L., Karl, T., Glasius, M., Guenther, A., Goldstein, A.
837 H., Seinfeld, J. H., Gold, A., Kamens, R. M., and Surratt, J. D.: Organosulfates as tracers for secondary organic aerosol (SOA)
838 formation from 2-methyl-3-buten-2-ol (MBO) in the atmosphere, Environ. Sci. Technol., 46, 9437-9446, doi:
839 10.1021/es301648z, 2012.
840 Zhang, H., Zhang, Z., Cui, T., Lin, Y. H., Bhathela, N. A., Ortega, J., Worton, D. R., Goldstein, A. H., Guenther, A., Jimenez, J. L.,
841 Gold, A., and Surratt, J. D.: Secondary organic aerosol formation via 2-methyl-3-buten-2-ol photooxidation: evidence of acid-
842 catalyzed reactive uptake of epoxides, Environ. Sci. Technol. Lett., 1, 242-247, doi: 10.1021/ez500055f, 2014.
843 Zhu, M., Jiang, B., Li, S., Yu, Q., Yu, X., Zhang, Y., Bi, X., Yu, J., George, C., Yu, Z., and Wang, X.: Organosulfur compounds
844 formed from heterogeneous reaction between SO_2 and particulate-bound unsaturated fatty acids in ambient air, Environ. Sci.
845 Technol. Lett., 6, 318-322, doi: 10.1021/acs.estlett.9b00218, 2019.
846
847

https://doi.org/10.5194/acp-2020-784
Preprint. Discussion started: 14 September 2020

Atmospheric Chemistry and Physics Discussions

848 **Table 1.** Organosulfates (in ng m^{-3}) quantified by UPLC-ESI(-)-QToFMS.

Category	m/z, $[M-H]^-$	Formula, $[M-H]^-$	Standards for quantification	Proposed structure	Ref.	Average concentration	
						2015/2016	2018/2019
Isoprene OS	167.0014	$C_4H_7O_5S^-$	Lactic acid sulfate (LAS)	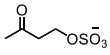	a	1.13	1.45
	182.9963	$C_4H_7O_6S^-$	LAS		b	2.84	2.19
	197.0120	$C_5H_9O_6S^-$	LAS	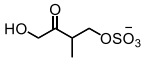	c	1.87	1.72
	198.9912	$C_4H_7O_7S^-$	LAS	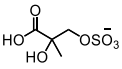	d	2.28	2.50
	199.0276	$C_5H_{11}O_6S^-$	LAS	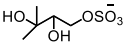	c	0.57	0.65
	210.9912	$C_5H_7O_7S^-$	LAS		d	6.09	4.81
	213.0069	$C_5H_9O_7S^-$	LAS		d	3.81	3.82
	215.0226	$C_5H_{11}O_7S^-$	LAS	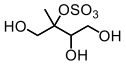	e	11.35	8.92
	237.0069	$C_7H_9O_7S^-$	LAS	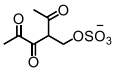	f	0.58	0.50
	260.0076	$C_5H_{10}NO_9S^-$	LAS	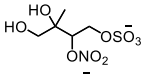	g	2.28	2.96
	273.9869	$C_5H_8NO_{10}S^-$	LAS	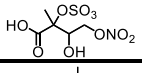	h	1.89	4.87
Monoterpene OS	223.0276	$C_7H_{11}O_6S^-$	Glycolic acid sulfate (GAS)	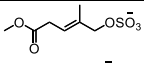	i	1.37	1.12
	239.0225	$C_7H_{11}O_7S^-$	GAS	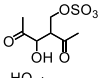	f	1.91	2.01
	249.0797	$C_{10}H_{17}O_5S^-$	α-Pinene sulfate		j	0.33	0.17
	251.0589	$C_9H_{15}O_6S^-$	Limonaketone sulfate		j	1.32	1.02
	253.0382	$C_8H_{13}O_7S^-$	GAS	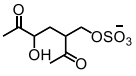	a	1.39	1.73
	279.0538	$C_{10}H_{15}O_7S^-$	GAS	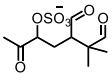	g	2.99	4.00
	281.0695	$C_{10}H_{17}O_7S^-$	α-Pinene sulfate	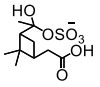	f	0.34	0.21
	294.0648	$C_{10}H_{16}NO_7S^-$	α-Pinene sulfate	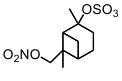	k	6.21	5.55

https://doi.org/10.5194/acp-2020-784
Preprint. Discussion started: 14 September 2020

Atmospheric Chemistry and Physics Discussions

	296.0440	$C9H14NO_8S^-$	Limonaketone sulfate	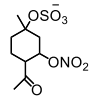	k	1.62	2.29
	342.0495	$C10H16NO_{10}S^-$	Limonaketone sulfate	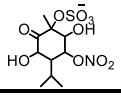	i	1.32	1.59
Anthropogenic OS	151.0065	$C_4H_7O_4S^-$	Methyl sulfate	unknown	–	2.04	1.80
	194.9963	$C_5H_7O_6S^-$	GAS	unknown	–	0.83	0.76
	209.0120	$C_6H_9O_6S^-$	GAS	unknown	–	1.44	0.63
	209.0845	$C_8H_{17}O_4S^-$	Sodium octyl sulfate	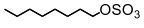	–	1.04	0.86
	172.9909	$C_6H_5O_4S^-$	Phenyl sulfate		l	0.36	0.12
	187.0065	$C_7H_7O_4S^-$	Phenyl sulfate	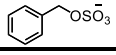	l	0.35	0.17
C_2/C_3 OS	136.9909	$C_3H_5O_4S^-$	GAS	unknown	–	0.62	0.50
	138.9701	$C_2H_3O_5S^-$	GAS		g	0.58	0.57
	152.9858	$C_3H_5O_5S^-$	GAS		d	2.30	1.79
	154.9650	$C_2H_3O_6S^-$	GAS	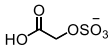	m	2.91	2.25
	155.0014	$C_3H_7O_5S^-$	GAS		n	1.21	0.70
	168.9807	$C_3H_5O_6S^-$	LAS	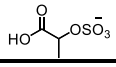	m	2.24	1.94
Unknown source OS	164.9858	$C_4H_5O_5S^-$	Methyl sulfate		n	1.20	0.78
	241.9971	$C_5H_8NO_8S^-$	Methyl sulfate	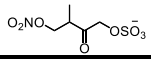	n	1.67	1.21
SUM						**65.48**	**59.04**

References for proposed OS structures: [a] Schindelka et al. (2013)), [b] Shalamzari et al. (2013), [c] Riva et al. (2016a), [d] Hettiyadura et al. (2015), [e] Surratt et al. (2010), [f] Nozière et al. (2010), [g] Surratt et al. (2007a) , [h] Nestorowicz et al. (2018), [i] Yassine et al. (2012), [j] Wang et al. (2017), [k] Surratt et al. (2008), [l] Huang et al. (2018), [m] Olson et al. (2011), [n] Hettiyadura et al. (2019).

Table 2. A summary of OS concentration (in ng m^{-3}) and its contribution to OM (OS/OM) in four seasons in 2015/2016 and 2018/2019.

Season	2015/2016		2018/2019	
	OS	OS/OM	OS	OS/OM
All year	65.5±77.5	0.57%±0.56%	59.4±79.7	0.66%±0.56%
Spring	51.1±24.4	0.34%±0.10%	51.5±28.8	0.48%±0.15%
Summer	114.1±128.4	1.13%±0.78%	102.1±137.7	1.18%±0.81%
Autumn	38.2±21.7	0.36%±0.11%	38.0±20.0	0.54%±0.24%
Winter	44.5±17.5	0.32%±0.12%	37.3±18.4	0.36%±0.13%

https://doi.org/10.5194/acp-2020-784
Preprint. Discussion started: 14 September 2020

Atmospheric Chemistry and Physics Discussions

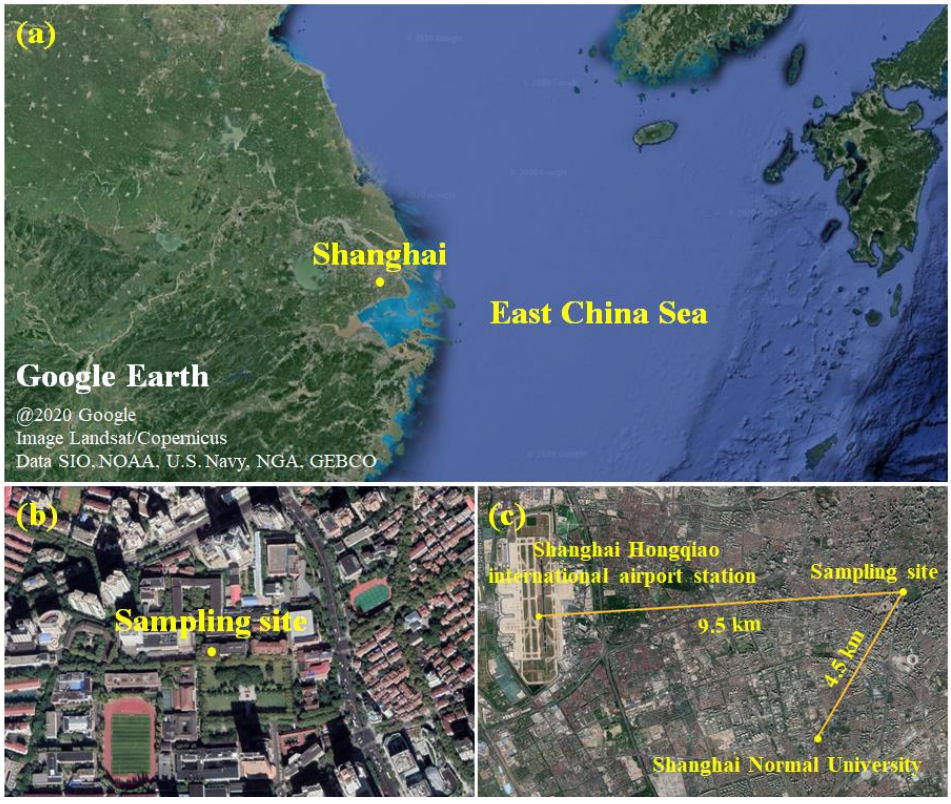

Figure 1. (a) Map of Shanghai. **(b)** Map of the sampling site on the Xuhui Campus of Shanghai Jiao Tong University in downtown. **(c)** Map of the $PM_{2.5}$ sampling site, the meteorological station at Shanghai Hongqiao international airport, the air quality monitoring station at Shanghai Normal University, and distances between them.

https://doi.org/10.5194/acp-2020-784
Preprint. Discussion started: 14 September 2020

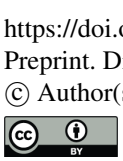

Atmospheric Chemistry and Physics Discussions

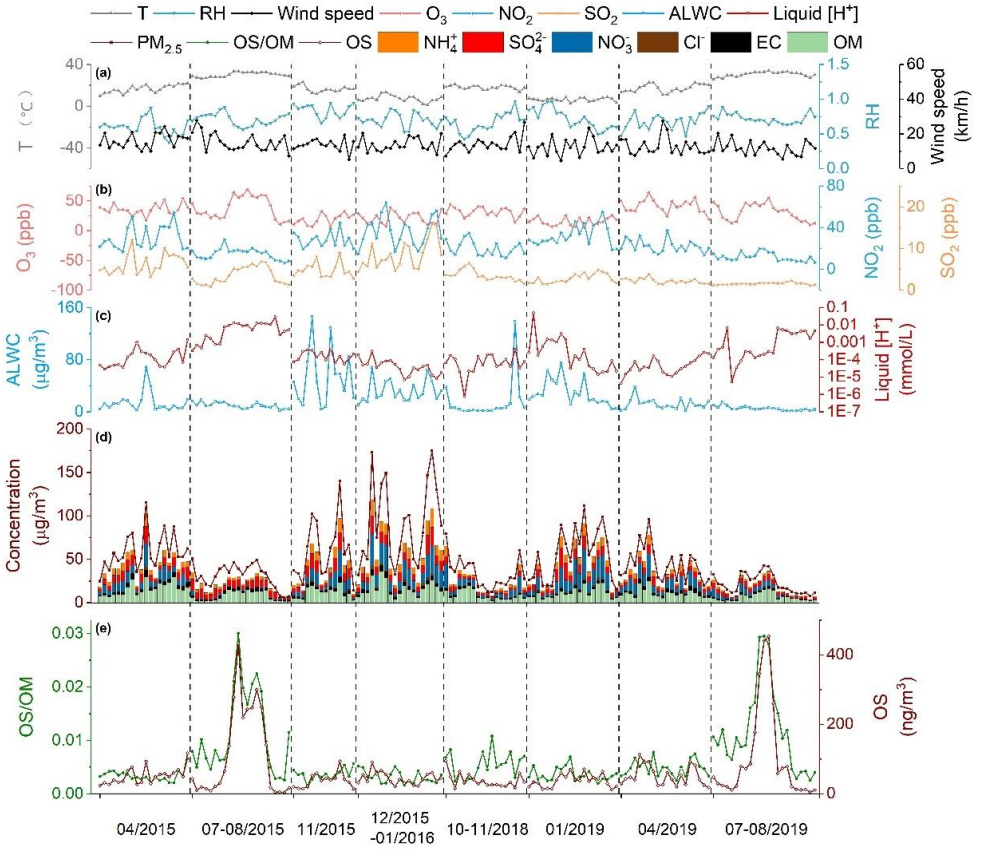

Figure 2. Time series of temperature, relative humid (RH), wind speed, O_3, NO_2, SO_2, aerosol liquid water content (ALWC) and liquid [H^+], concentrations of particulate organic matter (OM), elemental carbon (EC), sulfate, nitrate, chloride, ammonium, as well as the abundance of OS and its contribution to OM in 2015/2016 and 2018/2019 in Shanghai.

https://doi.org/10.5194/acp-2020-784
Preprint. Discussion started: 14 September 2020

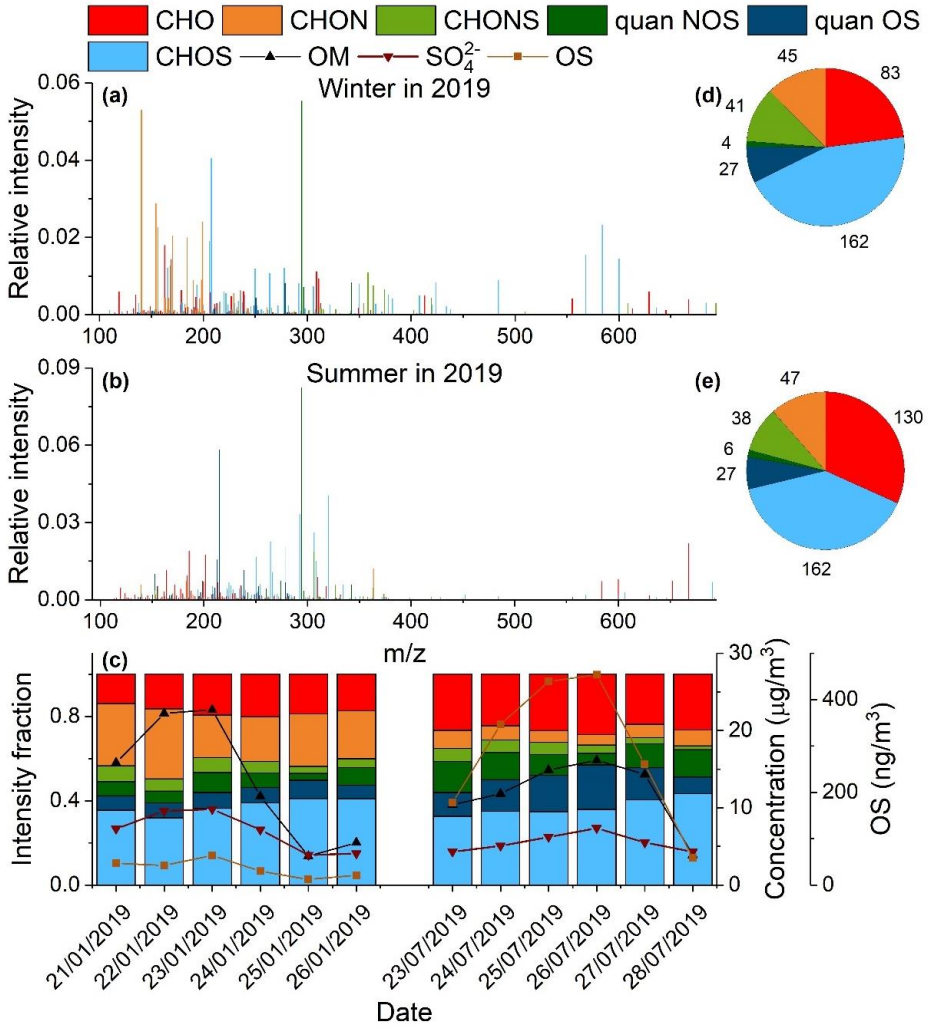

Figure 3. Average mass spectra of detected compounds in ambient aerosols during typical **(a)** wintertime (21-26 January 2019) and **(b)** summertime (23-28 July 2019) pollution episodes in Shanghai. The detected compounds were classified into six categories, i.e., CHO, CHON, CHOS, CHONS, quantified NOS, and quantified OS. The CHOS and CHONS categories excluded quantified OS and NOS, respectively. **(c)** The intensity fraction of different compound categories, as well as the time series of OM, SO_4^{2-}, and OS concentrations during two pollution episodes in 2019. **(d) (e)** The number of compounds detected in each category during the pollution episodes in winter and summer, respectively.

https://doi.org/10.5194/acp-2020-784
Preprint. Discussion started: 14 September 2020

Atmospheric Chemistry and Physics Discussions

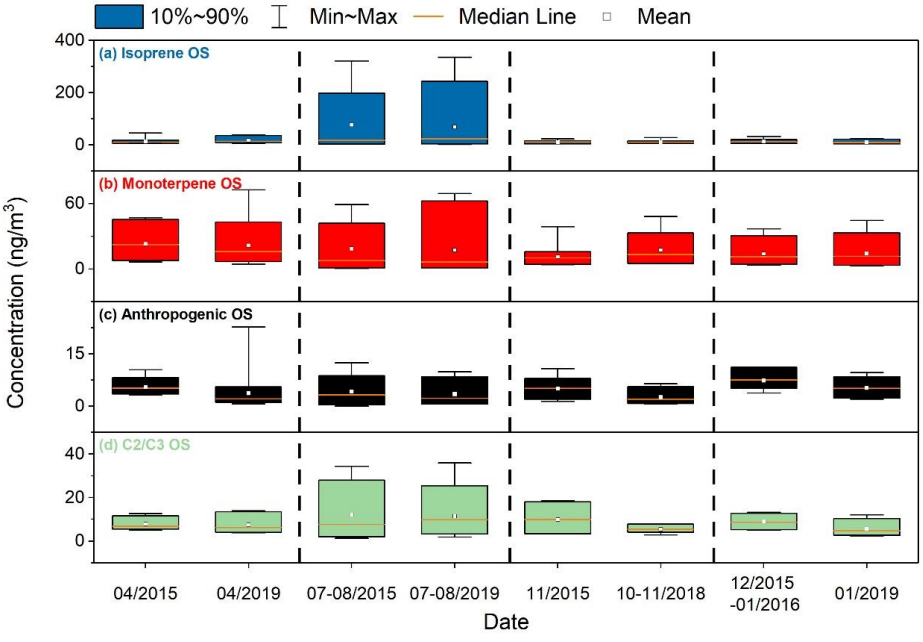

877

878 **Figure 4.** The concentrations of different types of the quantified OS over four seasons in 2015/2016 and 2018/2019.

879

https://doi.org/10.5194/acp-2020-784
Preprint. Discussion started: 14 September 2020

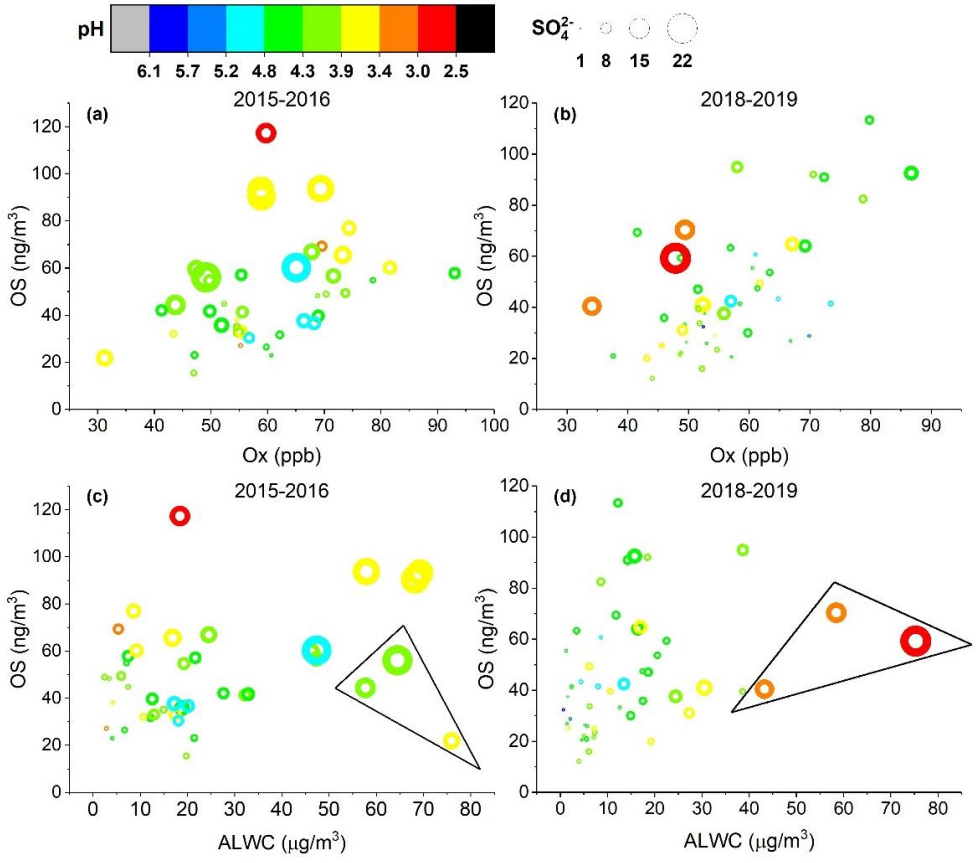

Figure 5. The quantified OS concentrations as a function of **(a) (b)** the Ox level and **(c)(d)** aerosol liquid water content (ALWC) in 2015/2016 and 2018/2019 except for summer. The circles are colored according to the aerosol pH, and their size is linearly scaled with the SO_4^{2-} concentration. The markers inside the triangle indicate the observations with low Ox levels (<50 ppb).

https://doi.org/10.5194/acp-2020-784
Preprint. Discussion started: 14 September 2020

Atmospheric Chemistry and Physics Discussions

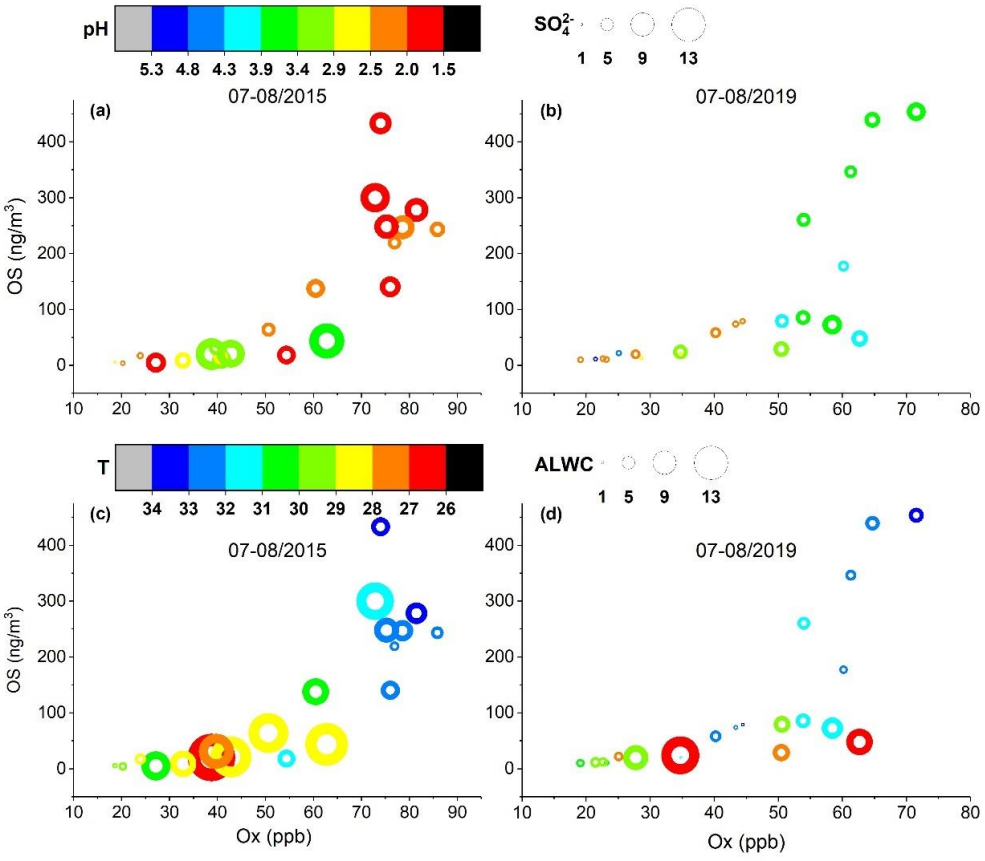

885

886 **Figure 6.** The quantified OS concentrations as a function of the Ox level in the summer of **(a) (c)** 2015 and **(b) (d)** 2019. The
887 color of circles in **(a) (b)** indicates the aerosol pH, and their size is linearly scaled with the SO_4^{2-} concentration. The color of
888 circles in **(c) (d)** indicates ambient temperature and their size is linearly scaled with aerosol liquid water content (ALWC)**.**

889

890